APPLICATION OF DENSITY FUNCTIONAL THEORY TO THE CALCULATION OF MOLECULAR CORE-ELECTRON BINDING ENERGIES

by

Germán Cavigliasso

B. Sc., Universidad Nacional de Córdoba (Argentina), 1995

A THESIS SUBMITTED IN PARTIAL FULFILLMENT OF THE REQUIREMENTS FOR THE DEGREE OF

MASTER OF SCIENCE

in

THE FACULTY OF GRADUATE STUDIES

DEPARTMENT OF CHEMISTRY

We accept this thesis as conforming to the required standard

THE UNIVERSITY OF BRITISH COLUMBIA

July 1999

In presenting this thesis in partial fulfilment of the requirements for an advanced degree at the University of British Columbia, I agree that the Library shall make it freely available for reference and study. I further agree that permission for extensive copying of this thesis for scholarly purposes may be granted by the head of my department or by his or her representatives. It is understood that copying or publication of this thesis for financial gain shall not be allowed without my written permission.

Department of Chemistry

The University of British Columbia
Vancouver, Canada

Date 20 July 1999

DE-6 (2/88)

Abstract

The procedure for calculating core-electron binding energies (CEBEs), based on the unrestricted generalized transition state (uGTS) model combined with density functional theory (DFT) employing Becke's 1988 exchange (B88) and Perdew's 1986 correlation (P86) functionals, which has proven to yield highly accurate results for C, N, O, and F cases, was extended to boron-containing molecules and to Si, P, S, Cl, and Ar cases.

Both unscaled and scaled basis sets were used in the studies of boron-containing molecules. The scaled-pVTZ basis set was as highly efficient for boron as it had been found to be for C, N, O, and F cases; the average absolute deviation (AAD) of the calculated CEBEs from experiment was 0.24 eV, compared to 0.23 eV for the much larger cc-pV5Z basis set. A generalization of the exponent-scaling methodology was proposed and tested on boron-containing molecules, and was found not to improve the original results to a significant extent.

The preliminary calculations of Si, P, S, Cl, and Ar CEBEs indicated that, in order to achieve the accuracy obtained for second-period elements, refinement of the basis sets and inclusion of relativistic effects are necessary.

As an additional application of the DFT/uGTS/scaled-pVTZ approach, the CEBEs of four isomers of C_3H_5NO were calculated. The distinctive nature of the core-ionization spectra of the isomers was depicted by the results, thus illustrating the potential utilization of accurate theoretical predictions

as a complement to electron spectroscopy for chemical analysis.

The model error in uGTS calculations and the errors in the functionals employed were calculated. It was observed that the high accuracy of the B88/P86 combination was due to a fortuitous cancellation of the functional and model errors. In view of this finding, a Kohn-Sham total-energy difference approach, which eliminates the model error, was investigated.

Ten functional combinations and several basis sets (including unscaled, scaled, and core-valence correlated functions) were tested using a database of reliable observed CEBEs. The functionals designed by Perdew and Wang (1986 exchange and 1991 correlation) were found to give the best performance with an AAD from experiment of 0.15 eV. The scaled basis sets did not perform as well as they did in the uGTS calculations, but it was found that the core-valence correlated cc-pCVTZ basis functions were an excellent alternative to the cc-pV5Z set as they provided equally accurate results and could be applied to larger molecules.

Table of Contents

Abstract ii

List of Tables vii

List of Figures xi

Preface xii

Acknowledgements xiii

1 Introduction 1

1.1 Core-Electron Binding Energies 3

1.1.1 Calculations of Core-Ionization Energies 5

1.2 Scope and Organization of this Thesis 7

2 Density Functional Theory in Quantum Chemistry 10

2.1 Traditional Ab Initio Quantum Chemistry 11

2.1.1 The Hartree-Fock Method 13

2.1.2 Electron Correlation 17

2.2 Density Functional Theory 19

2.2.1 The Kohn-Sham Formulation 21

2.2.2 Density Functionals 24
2.3 A Comparison between DFT and Traditional Methods 30
2.4 Computational Aspects of Quantum Chemical Methods 32
2.4.1 Basis Sets 34

3 Computational Approach 36
3.1 The uGTS and ΔE-KS Approaches 36
3.2 The Density Functional Program deMon 40
3.2.1 Basis Sets 41

4 Applications of the uGTS Model 48
4.1 Boron-Containing Molecules 49
4.2 Isomers of C_3H_5NO 57
4.3 Core-Electron Binding Energies of Si, P, S, Cl, and Ar 62

5 The ΔE-KS Approach: Test of Functionals 69
5.1 Model Error and Functional Error 71
5.2 Functional Performance in ΔE-KS Calculations 75

6 The ΔE-KS Approach: Test of Basis Sets 79
6.1 Scaled Basis Sets 80
6.2 Core-Valence Correlated Basis Sets 84

7 Conclusion 91

References 94

Appendix 108

List of Tables

3-1 Composition of cc-pVnZ basis sets 42

3-2 Scaling factors (uGTS) for second-period atoms 45

3-3 Scaling factors (ΔE-KS) for second-period atoms 46

4-1 Basis set convergence in the calculation of B 1s energies with unscaled basis sets 50

4-2 Calculations of B core-electron binding energies with scaled basis sets 51

4-3 Basis set convergence in the calculation of C, N, O, and F 1s energies with unscaled basis sets 52

4-4 Calculations of C, N, O, and F core-electron binding energies with scaled basis sets 53

4-5 Average Absolute Deviation and Maximum Deviation of calculated core-electron binding energies from experiment and from CBS 54

4-6 Calculations of core-electron binding energies with the gs-pVTZ basis set 56

4-7 Deviation analysis of the gs-pVTZ basis set performance for the 12 cases reported in Table 4-6 57

4-8 Total energies, relative energies with respect to ethyl isocyanate, and dipole moments for the isomers of C_3H_5NO 58

4-9 Core-electron binding energies for the isomers of C_3H_5NO 60

4-10 Basis set convergence in the calculation of Si $2p$ energies 63

4-11 Basis set convergence in the calculation of P $2p$ energies 64

4-12 Basis set convergence in the calculation of S $2p$ energies 65

4-13 Basis set convergence in the calculation of Ar and Cl $2p$ energies 66

4-14 Average Absolute Deviation of calculated core-electron binding energies from experiment sorted by element 67

4-18 Average Absolute Deviation of calculated core-electron binding energies from experiment for all test cases 68

5-1 Composition of exchange-correlation functionals 70

5-2 Error analysis for uGTS calculations with the B88/P86 functional 72

5-3 Error analysis for uGTS calculations with the P86/P86 functional 73

5-4 Error analysis for uGTS calculations with the LSD functional 74

5-5 Average Absolute Deviation and Maximum Deviation of the core-electron binding energies (calculated with the functionals in Table 5-1) from experiment 76

5-6 Core-electron binding energies calculated with the P86/P91 functional 77

6-1 Basis set convergence in ΔE-KS/P86-P91 calculations of core-electron binding energies 81

6-2 ΔE-KS/P86-P91 calculations of core-electron binding energies with scaled basis sets 82

6-3 Average Absolute Deviation of calculated core-electron binding energies from experiment and from CBS 83

6-4 ΔE-KS/P86-P91 calculations of core-electron binding energies with cc-pCVTZ basis sets 85

6-5 Average Absolute Deviation of calculated core-electron binding energies from experiment 86

6-6 Calculations of core-electron binding energies of larger molecules 87

A-1 Observed 1*s* energies for the molecules in the seventeen-case database 109

A-2 Observed 1s energies for the aromatic compounds in Table 6-6 114

A-3 Observed 1s energies for hydrogen fluoride 115

List of Figures

4-1 Numbering scheme for the isomers of C_3H_5NO 59

4-2 Calculated and available experimental CEBEs for the isomers of C_3H_5NO 61

6-1 Completeness profiles of cc-pVnZ and cc-pCVTZ basis sets 88

6-2 Comparison of completeness profiles for the s-, p-, and d-type functions of cc-pVTZ, cc-pV5Z, and cc-pCVTZ basis sets 89

Preface

Part of the results reported in this thesis have been published, accepted, or submitted for publication. The corresponding references are

- G. Cavigliasso, D. P. Chong, Accurate Density Functional Calculation of Core-Electron Binding Energies with a Scaled Polarized Triple-Zeta Basis Set. VI. Extension to Boron-Containing Molecules, *Can. J. Chem.*, 1999, 77-1, 24

- D. P. Chong, G. Cavigliasso, Density-Functional Calculation of Core-Electron Binding Energies of Isomers of $C_3H_6O_2$ and C_3H_5NO, *Int. J. Quantum Chem.*, accepted

- G. Cavigliasso, D. P. Chong, Accurate Density Functional Calculation of Core-Electron Binding Energies by a Total-Energy Difference Approach, *J. Chem. Phys.*, submitted

Most of the data contained in the Appendix were collected and organized by Prof. Delano P. Chong.

Acknowledgements

I would like to express my gratitude to all the people who have contributed to my academic experience at the University of British Columbia. I am much obliged to

Professor Del Chong, my research supervisor
Dr. Ching-Hang Hu
Professors Gren Patey and Mark Thachuk
Professors Elmer Ogryzlo and Robert Thompson

I am also grateful to the academic and administrative personnel of the Department of Chemistry at UBC, in particular the graduate secretaries Tilly Schreinders, Judy Wrinskelle and Diane Mellor, my instructors, classmates and research lab-mates.

I would like to acknowledge financial support from the Department of Chemistry, the Faculty of Science and the Faculty of Graduate Studies.

I dedicate this thesis to my teachers.

Chapter 1

Introduction

The roots of Density Functional Theory (DFT) date back to the days when quantum mechanics was in its early stages of development [1]. It was, however, the work of Hohenberg, Kohn, and Sham [2, 3] in the 1960s that rigorously established density functional theory as a legitimate method of describing the electronic structure of matter.

Applications of DFT to electronic structure calculations concentrated initially on solid-state systems and on problems which were of interest especially to physicists. The impact that DFT has had on theoretical and computational solid-state physics has been extremely significant as summarized by the remarks of Fulde [4] — " (DFT) has given (electronic structure) calculations a sounder theoretical basis than they had previously " — and Kohn [5] — " (DFT) vitalized first researches in the electronic structure of simple crystals and subsequently those on more complex systems (such as) defects,

alloys, surfaces, superconductivity, magnetism ".

Although the incorporation of density functional methods into the field of quantum chemistry (and computational molecular science in general) did not occur as rapidly as it had in the case of solid-state physics, over the past two decades there have been ever-increasing numbers of applications to chemical systems, applications which have been supported by continuing advances in both theoretical methodology and computational implementation [6–15]. Density functional calculations have become a highly effective method for studying the structure, properties, and dynamics of a wealth of molecular systems, and have been developed to a level where they challenge the accuracy of the conventional (more "sophisticated") quantum chemical techniques, which they already surpass in terms of computational efficiency and applicability to relatively large systems [16]. Density functional theory is also highly appealing, from a conceptual point of view, in that several important universal concepts of molecular structure and reactivity — such as chemical potential, electronegativity, hardness and softness, reactivity indices — are naturally involved in the density functional language [1, 9, 11, 15].

In an article entitled " The reachable dream: some steps toward the realization of quantum mechanics by computer " [17], Schaefer pointed out that "the dream" was in part " to make computational quantum chemistry sufficiently efficient and indispensable that experimental chemists would employ it routinely, much as they use NMR spectroscopy ". Density functional theory is playing and will continue to play a leading role in the realization of Schaefer's dream; the principal reason has been clearly stated by Ziegler

[7], " ... popularity of approximate DFT stems in large measure from its computational expedience which makes it amenable to large-size or real-life molecules ... ".

The determination of core-electron binding energies (CEBEs) is one of the molecular problems which recently has been successfully addressed by density functional calculations [18-29]. The purpose of this work is to extend the applications of DFT to the calculation of molecular CEBEs by studying some additional systems with the already established methodology and by exploring new computational approaches.

1.1 Core-Electron Binding Energies

The binding energy (E_B) of an electron in a core level is the difference between the total energies of the initial (E_i^N) and final (E_f^{N-1}) states of the system, the former being the neutral molecule and the latter being a singly ionized cation (created by removal of the inner-shell electron) [30, 31],

$$E_B = E_f^{N-1} - E_i^N \tag{1.1}$$

where N is the total number of electrons. Binding energies of core electrons are determined experimentally by X-ray Photoelectron Spectroscopy (XPS) [30–32] according to the relation [33]

$$K_E = h\nu - E_B \tag{1.2}$$

where K_E is the kinetic energy of an electron that has been ejected by an X-ray photon of energy $h\nu$.

Core-ionization energies have been widely used for analytical purposes. The technique is known as Electron Spectroscopy for Chemical Analysis (ESCA) and utilizes data for electron binding energies as a means of determining elemental composition and of providing structural information via the so-called chemical shifts [30–33]. ESCA has proven useful for solid-state and surface science studies [30, 34–36] because the small escape depth for electrons renders it particularly suited to probing the outermost atomic layers of a solid-state material and also the adsorption of atoms or molecules on a surface.

In addition to the practical uses of CEBE data, much attention has been focused on the chemical shifts for more fundamental reasons. A chemical shift is defined as a change in the CEBE of an atom due to a modification of its chemical environment [30–33]. In this sense, the analysis and understanding of chemical shifts constitute a valuable means of gaining insight into properties of significant chemical interest (such as the nature of chemical bonds in a molecule or solid). Some examples of investigations that have pursued this direction are the combination of core and valence ionization potential data to quantify the bonding or antibonding character of molecular orbitals [37–40], exploration of the connections between CEBEs and the concept of resonance [41] and of the correlation of CEBEs with activation energies for addition reactions to alkenes [42], and studies of electronic substituent effects in iron complexes of aromatic molecules [43].

1.1.1 Calculations of Core-Ionization Energies

Core-electron spectroscopy has been recognized as a " field of research for which the interplay between theory and experiments has been of particular importance " [44]. Calculations of the binding energies of core electrons and of their chemical-environment-dependent shifts have proven useful in assisting the interpretation and understanding of various aspects of core-level ionization phenomena [26–28, 44–52].

A rigorous theoretical approach to determining CEBEs involves performing separate total-energy calculations for both the initial ground-state and the final core-hole state of equation (1.1). This total-energy difference procedure was introduced by Bagus [53] and has been applied [46, 48, 49, 54–57] mainly at the Hartree-Fock level of theory (Chapter 2), but also considerably more sophisticated (and computationally expensive) quantum chemical calculations have been reported, including configuration interaction [46, 58], multiconfiguration [49], and second-order perturbation theory [49] investigations. Some calculations have employed the equivalent-core approximation — first introduced by Shirley [59] — in which the exact calculation of the core-hole state is replaced by a ground-state calculation of the equivalent system obtained by increasing the nuclear charge on the atom being ionized by one unit.

The Hartree-Fock total-energy difference procedure — most frequently referred to as the ΔSCF method — has not been particularly good at estimating absolute CEBEs, but has been remarkably good at predicting accurate values for the chemical shifts [48, 49]. Because the computational demands of high-quality quantum chemistry render the application of the total-energy

difference method to even moderately-sized molecules and clusters (which are widely used as models for surfaces) impractical, and because most of the interest has focused on the chemical shifts (rather than the absolute CEBEs), several alternative models and methods have been devised [44, 54, 60, 61]. Some are specifically designed to avoid performing the core-ionized cation calculations, and have been employed extensively, often yielding good quantitative results [61].

Approaches that take advantage of Slater's transition state concept [62] — and thus rely on the use of fractional orbital occupation numbers to calculate absolute CEBEs — have also been proposed as an alternative to the procedures that require calculations on fully ionized final states. Following this line, Chong and coworkers [63–65] applied a transition-operator-moment/perturbation-theory approach with encouraging success (average deviation from experiment was 0.4 eV for eight cases involving small molecules [65]) but the computational effort was still too expensive for the method to be extended to larger systems.

With the evolution of density functional theory into an accurate and reliable quantum chemical technique, applications of DFT-based methods to core-ionization phenomena have been actively pursued. Approaches that make use of the transition state model [47, 66], the total-energy difference procedure [67], and of combinations of calculations with observed data [68] have been employed, and they have been successfully applied to both discrete [47] and extended [66–68] systems.

Chong [18, 19] has recently introduced methodology based on a combination of DFT with the generalized transition state model [69] — an exten-

sion of Slater's original transition state idea — and has extensively tested [18–29] it on a wide variety of systems, including both closed-shell and open-shell small molecules, transition metal complexes, and also model systems for polymers and adsorbate-surface interactions. High quantitative accuracy has been accomplished (average deviations from experiment of 0.2 eV or lower have been routinely achieved [19, 20, 24, 27, 28, 29]) and the procedure has also proven useful from a qualitative point of view. For example, investigations of the CEBEs of isomers of C_2H_4O, C_3H_3NO, and C_6H_6 [20, 29] have provided results which support the possible use of electron spectroscopy for chemical analysis. Also, surface-science-oriented studies have shown that employing CEBEs for the interpretation of XPS spectra on a molecular scale constitutes a useful method for tracing the interactions of molecules with a surface [26], and is of valuable assistance in the interpretation of XPS spectra of compounds for which there is no gas-phase reference spectrum [27]. These examples support and confirm the significance of the role played by computational techniques in the aforementioned theory-experiment interplay in core-electron spectroscopy.

1.2 Scope and Organization of this Thesis

This thesis consists of seven chapters, which fall into two groups: background and reference material (Chapters 1, 2, and 3), and presentation and discussion of results (Chapters 4, 5, 6, and 7).

Chapter 2 contains material of a theoretical nature which is intended to serve as introductory-level background to density functional theory and how

it relates to and differs from more conventional ab initio quantum chemical methods. Chapter 3 will present a description of the computational approach, including the mathematical formalism, and some details of the calculation code and the basis sets employed.

The density functional investigations of Chong and coworkers have addressed a large number of cases of core-electron binding energies of the second-period elements carbon, nitrogen, oxygen, and fluorine. All the studies have employed the unrestricted Generalized Transition State (uGTS) model [18]. Part of the work reported in this thesis was devoted to extending the applications of the uGTS/DFT approach to the calculation of molecular CEBEs. Thus, Chapter 4 will present the results of a study of core-ionization energies of boron-containing molecules, and of the third-period elements silicon, phosphorus, sulphur, chlorine, and argon. Also in Chapter 4, an investigation of the CEBEs of isomers of C_3H_5NO, which explores the analytical applications of core-electron spectroscopy, will be reported.

Chapters 5 and 6 contain the results of a different approach to the determination of CEBEs which is based on a density functional total-energy difference (ΔE) procedure. An error-based comparison between the uGTS and the ΔE methods, and a test of functionals for use within the latter approach will be presented in Chapter 5, whereas the results of tests of various basis sets will be the subject of Chapter 6.

All the calculated core-electron binding energies reported in this thesis are vertical ionization potentials in the sense that the calculations were carried out at the equilibrium geometries of the neutral molecules for both the initial state (neutral species) and the final state (ionized species) [48]. The results

obtained will be almost exclusively discussed and analyzed in terms of comparisons of calculation with experiment, and the extent of their agreement with the observed values will be the major factor in assessing the performance of the computational procedures.

Chapter 2

Density Functional Theory in Quantum Chemistry

" A primary objective of molecular quantum mechanics is the solution of the non-relativistic, time-independent Schrödinger equation, and in particular the calculation of the electronic structures of atoms and molecules " [70]. In order to achieve the goal of calculating molecular electronic structure, two main approaches are widely employed. Semiempirical methods [70–72] introduce a number of significant approximations in the solution of the Schrödinger equation, and rely upon adjustable parameters obtained from experimental information; their use is limited to the chemical systems for which they were parameterized. Methods which do not resort to empirical data (except for the use of values of fundamental constants and nuclear atomic numbers) are in principle applicable to any molecular system, and are generally divided into traditional ab initio [73] and density functional [1, 74] approaches. In the former, the wavefunction is central to the description

of electronic structure, whereas in the latter the electron density plays the major role.

In this chapter, a description of the principal concepts of density functional theory and quantum chemistry will be presented, and some of the similarities and differences between DFT and traditional quantum chemistry will be discussed.

2.1 Traditional Ab Initio Quantum Chemistry

The study of the behaviour and properties of electrons in molecules requires the solution of the time-independent Schrödinger equation which has the general eigenvalue-problem form [70, 73]

$$\hat{H}\,\Phi = E\,\Phi \tag{2.1}$$

where Φ is the wavefunction, E is the total energy, and $\hat{H}$ is the (non-relativistic) Hamiltonian operator, given by

$$\hat{H} = \hat{T}_{nuc} + \hat{T}_{el} + \hat{U}_{nuc} + \hat{V}_{ext} + \hat{U}_{ee} \tag{2.2}$$

The terms on the right-hand side of equation (2.2) have the following physical interpretations and mathematical expressions (in atomic units [73]):

$\hat{T}_{nuc} = -\sum_A \frac{1}{2M_A}\nabla_A^2$ is the nuclear kinetic energy operator,

$\hat{T}_{el} = -\sum_i \frac{1}{2}\nabla_i^2$ is the electronic kinetic energy operator,

$\hat{U}_{nuc} = \sum_A \sum_{B>A} \frac{Z_A Z_B}{R_{AB}}$ is the potential energy operator for nuclear repulsions,

$\hat{V}_{ext} = -\sum_i \sum_A \frac{Z_A}{r_{iA}}$ is the potential energy operator for electron-nucleus attractions,

$\hat{U}_{ee} = \sum_i \sum_{j>i} \frac{1}{r_{ij}}$ is the potential energy operator for electron-electron repulsions.

In the above expressions, M_A is the ratio of the mass of nucleus A to the mass of an electron, Z_A is the atomic number of nucleus A, ∇_A^2 and ∇_i^2 are Laplacian operators [75] for nucleus A and electron i respectively, and $r_{ij} = |\mathbf{r}_i - \mathbf{r}_j|$, $r_{iA} = |\mathbf{r}_i - \mathbf{R}_A|$, $R_{AB} = |\mathbf{R}_A - \mathbf{R}_B|$, where $\mathbf{r}$ and $\mathbf{R}$ are electronic and nuclear position vectors, respectively.

Solving the Schrödinger equation is a formidable task even for the simplest molecular systems, so a number of approximations must be introduced to make calculations feasible. The vast majority of quantum chemical calculations are carried out within the Born-Oppenheimer approximation [76], which is based on the fact that electrons, being much lighter than nuclei, move considerably faster than nuclei do. Hence, it is reasonable to assume that electrons in molecules move in the field generated by fixed nuclei. This separation of the motion of electrons and nuclei leads to the "electronic" Schrödinger equation

$$\hat{H}_{el}\Psi_{el} = (\hat{T}_{el} + \hat{V}_{ext} + \hat{U}_{ee})\Psi_{el} = E_{el}\Psi_{el} \tag{2.3}$$

where Ψ_{el} is the wavefunction describing the behaviour of the electrons. Both Ψ_{el} and the electronic energy E_{el} depend parametrically on nuclear positions.

A common quantum chemical solution to equation (2.3) utilizes the variational principle [73]. Given a trial (almost always approximate) wavefunction Ψ for a particular molecular system, the expectation value of the energy (E) will be greater than or equal to the true ground-state energy (E_0), $E \geq E_0$, or equivalently,

$$\frac{<\Psi|\hat{H}|\Psi>}{<\Psi|\Psi>} \geq \frac{<\Psi_0|\hat{H}|\Psi_0>}{<\Psi_0|\Psi_0>} \tag{2.4}$$

where Dirac notation [73] has been used. The equality holds only when Ψ is equivalent to the correct ground-state wavefunction Ψ_0.

2.1.1 The Hartree-Fock Method

The Hartree-Fock (HF) approximation is a mean-field method applied to the many-body electronic problem [16, 73, 77]. The central idea of the HF approach is the assumption that electrons move independently of one another and that a given electron interacts with an average field produced by the rest of the electrons. Therefore, an explicit treatment of the instantaneous pairwise interaction, the so-called electron correlation, is lacking.

For an N-electron system, an antisymmetrized product of N spin-orbitals (ψ_i), known as a Slater determinant, represents the simplest trial wavefunc-

tion which is physically acceptable. This determinant satisfies the Pauli Principle [73], a necessary condition, and is given by

$$\Psi_{HF} = \frac{1}{(N!)^{1/2}} \begin{vmatrix} \psi_1(\mathbf{x}_1) & \psi_2(\mathbf{x}_1) & \cdots & \psi_N(\mathbf{x}_1) \\ \psi_1(\mathbf{x}_2) & \psi_2(\mathbf{x}_2) & \cdots & \psi_N(\mathbf{x}_2) \\ & \vdots & & \\ \psi_1(\mathbf{x}_N) & \psi_2(\mathbf{x}_N) & \cdots & \psi_N(\mathbf{x}_N) \end{vmatrix} \tag{2.5}$$

The spin-orbitals in equation (2.5) are each a product of a spatial orbital $\varphi_i(\mathbf{r})$ and a spin function $\sigma(s)$ with $\sigma(s)$ being either $\alpha(s)$ for "spin-up" or $\beta(s)$ for "spin-down", and $\mathbf{x}$ indicating both space ($\mathbf{r}$) and spin (s) coordinates. They are generally orthonormal, that is

$$< \psi_i | \psi_j >= \delta_{ij} \tag{2.6}$$

so that the wavefunction is also normalized

$$< \Psi_{HF} | \Psi_{HF} >= 1 \tag{2.7}$$

The HF ground-state energy E_{HF} is obtained by a variational minimization of the expectation value of the electronic Hamiltonian of equation (2.3) with the wavefunction of equation (2.5) [73]. This procedure involves optimization of the spin-orbitals that comprise the Slater determinant and yields the Hartree-Fock equations

$$\hat{f}\psi_i = \epsilon_i \psi_i \tag{2.8}$$

where ϵ_i is the orbital energy and $\hat{f}$ is an effective one-electron operator known as the Fock operator, given by

$$\hat{f} = \hat{h} + \hat{v}^{HF} \tag{2.9}$$

The operator $\hat{h}$ is defined as

$$\hat{h}_i = -\sum_i \frac{1}{2}\nabla_i^2 - \sum_A \frac{Z_A}{r_{iA}} \tag{2.10}$$

and the effective one-electron HF potential operator $\hat{v}^{HF}$ is given by a sum of Coulomb ($\hat{J}$) and exchange ($\hat{K}$) contributions, that is

$$\hat{v}^{HF} = \sum(\hat{J} - \hat{K}) \tag{2.11}$$

The definitions of the Coulomb and exchange operators are

$$\hat{J}_j\psi_i = \left[\int \psi_j^*(\mathbf{x}_2)\psi_j(\mathbf{x}_2)\frac{1}{r_{12}}d\mathbf{x}_2\right]\psi_i(\mathbf{x}_1) \tag{2.12}$$

$$\hat{K}_j\psi_i = \left[\int \psi_j^*(\mathbf{x}_2)\psi_i(\mathbf{x}_2)\frac{1}{r_{12}}d\mathbf{x}_2\right]\psi_j(\mathbf{x}_1) \tag{2.13}$$

$\hat{K}_j$ is a non-local operator in the sense that the result of operating with it on an orbital $\psi_i(\mathbf{x}_1)$ depends on the value of ψ_i throughout all space, not just at $\mathbf{x}_1$ [73]. There are an infinite number of spin-orbitals which solve equation (2.8), so the N-electron HF ground-state wavefunction is formed from the N orbitals with the lowest energies, which are called the occupied spin-orbitals.

The HF ground-state energy is then given by

$$E_{HF} =< \Psi_{HF}|\hat{H}_{el}|\Psi_{HF} >= \sum_i H_i + \frac{1}{2}\sum_{i,j}(J_{ij} - K_{ij}) \tag{2.14}$$

where

$$H_i =< \psi_i|\hat{h}|\psi_i > \tag{2.15}$$

$$J_{ij} =< \psi_i|\hat{J}|\psi_j > \tag{2.16}$$

$$K_{ij} =< \psi_i|\hat{K}|\psi_j > \tag{2.17}$$

If the spin functions are integrated out in equations (2.16) and (2.17), then J_{ij} and K_{ij} can be expressed as functions of the spatial orbitals φ_i [73]. The resulting "spatial" J_{ij} contributions may be thought of as originating from the classical Coulomb repulsion between two charge clouds. However, no simple classical interpretation can be associated with the exchange K_{ij} contributions.

The energy of an individual spin-orbital is given by

$$\epsilon_i = H_i + \sum_j (J_{ij} - K_{ij}) \tag{2.18}$$

so the HF energy can be also expressed as

$$E_{HF} = \sum_i \epsilon_i - \frac{1}{2}\sum_{i,j}(J_{ij} - K_{ij}) \tag{2.19}$$

which shows that the individual orbital energies do not add up to the total electronic energy of the system. Instead, a physical interpretation can be given to ϵ_i by means of Koopmans' theorem [73], which states that the ionization potential (IP) for removal of an electron from a spin-orbital ψ_i in an N-electron HF wavefunction is the negative of the energy of the spin-orbital, that is

$$IP = -\epsilon_i \tag{2.20}$$

Due to the approximate nature of the Hartree-Fock model, ionization potentials determined according to (2.20) are only of a qualitative or semi-quantitative value [54].

2.1.2 Electron Correlation

The Hartree-Fock method is the simplest of the wavefunction-based approaches to molecular electronic structure, but it fails to provide a complete physical description of the many-electron problem because it disregards electron correlation.

The correlation energy is defined in conventional quantum chemistry as the difference between the exact non-relativistic ground-state energy E_0 (within the Born-Oppenheimer approximation) and the HF energy, that is

$$E_{corr} = E_0 - E_{HF} \tag{2.21}$$

An exact procedure exists for representing any state of an N-electron system, called Configuration Interaction (CI) [73]. The infinite number of spin-orbitals that are obtained as solutions to the HF equations can be viewed as two distinct sets of orbitals: the N lowest-energy occupied orbitals and the remaining higher-energy unoccupied or virtual orbitals. The former group is used to construct the ground-state wavefunction within the HF approximation while the latter group provides a means of generating excited configurations by promoting electrons from occupied to virtual orbitals. An exact N-electron wavefunction can be expressed as a linear combination of an infinite number of N-electron configurations (each represented by a Slater determinant), that is

$$\Psi_{exact} = c_0\Psi_0 + c_a^r \sum_{ra} \Psi_a^r + c_{ab}^{rs} \sum_{a<b, r<s} \Psi_{ab}^{rs} + \cdots \tag{2.22}$$

where Ψ_0 is the HF ground-state wavefunction, Ψ_a^r is a singly-excited configuration, Ψ_{ab}^{rs} is a doubly-excited configuration, and so on. The c's are expansion coefficients, the indices a and b label occupied orbitals, and the indices r and s label virtual orbitals.

In practice, it is impossible to handle infinite numbers of spin-orbitals and configurations, yet due consideration of electron correlation is necessary to improve upon the HF description. Therefore, a number of methods [4, 16, 73, 77] which employ different approximate approaches to the treatment of correlation effects have been developed. They include several approximate versions

of the CI method, the Multiconfigurational Self-consistent Field (MCSCF) method, the Coupled-Cluster (CC) method, and many-body perturbation techniques such as the Møller-Plesset Perturbation (MPPT) method.

2.2 Density Functional Theory

The fundamental variable of density functional theory is the electron density, ρ [1]. For a given state of an electronic system, the electron density is defined as the number of electrons per unit volume, and is mathematically represented in terms of the N-electron wavefunction Ψ by

$$\rho(\mathbf{r}_1) = N \sum_{spin} \int |\Psi(\mathbf{r}_1, \mathbf{r}_2, \cdots, \mathbf{r}_N)|^2 \, d\mathbf{r}_2 \cdots d\mathbf{r}_N \tag{2.23}$$

The electron density is thus a simple non-negative function of three variables (compared with 3N variables in the case of the N-electron wavefunction) which integrates to the total number of electrons N, that is

$$\int \rho(\mathbf{r}) \, d\mathbf{r} = N \tag{2.24}$$

A non-negative, continuous electron density that satisfies equation (2.24) is said to be N-representable [1].

A definitive proof that the electron density could play the central role in the description of the electronic structure of matter was given by Hohenberg and Kohn [2] in the form of two theorems.

The first theorem considers a system of N interacting electrons in a non-degenerate ground-state under the influence of an external potential $v(\mathbf{r})$

(which is not restricted to Coulomb potentials) and states that the ground-state density $\rho(\mathbf{r})$ uniquely determines $v(\mathbf{r})$, to within an additive constant. The number of electrons N is also determined by $\rho(\mathbf{r})$ via equation (2.24). Therefore, the electron density completely determines the Hamiltonian and, consequently, all properties of the system.

For a given external potential, the energy functional is

$$E[\rho] = V[\rho] + F_{HK}[\rho] \tag{2.25}$$

where

$$V[\rho] = \int \rho(\mathbf{r})\, v(\mathbf{r})\, d\mathbf{r} \tag{2.26}$$

and

$$F_{HK}[\rho] = T_{el}[\rho] + U_{ee}[\rho] \tag{2.27}$$

From equations (2.26) and (2.27) it follows that F_{HK} is a universal functional of the electron density, its form not being affected by the nature of the system.

The second Hohenberg-Kohn theorem makes it possible to find the ground-state density by means of a variational minimization search. It states that given an N-representable trial density ρ_{trial},

$$E[\rho_{trial}] \geq E_0 \tag{2.28}$$

The true ground-state energy E_0 is obtained only if the true ground-state

density is used as the trial density.

The search for $\rho(\mathbf{r})$ must be conducted subject to the constraint imposed by equation (2.24), that is

$$\delta\left\{E[\rho] - \mu\left[\int \rho(\mathbf{r})\, d\mathbf{r} - N\right]\right\} = 0 \tag{2.29}$$

The multiplier μ is the chemical potential, and is defined by [1]

$$\mu = \frac{\delta E[\rho]}{\delta \rho(\mathbf{r})} = v(\mathbf{r}) + \frac{\delta F_{HK}[\rho]}{\delta \rho(\mathbf{r})} \tag{2.30}$$

Provided the exact $F_{HK}[\rho]$ is known, equation (2.29) yields the exact ground-state electron density. As stated by Hohenberg and Kohn in their original paper [2]: " if $F[\rho]$ were a known and sufficiently simple functional of ρ, the problem of determining the ground-state energy and density in a given external potential would be rather easy since it requires merely the minimization of a functional of the three-dimensional density function. The major part of the complexities of the many-electron problems are associated with the determination of the universal functional $F[\rho]$ ".

2.2.1 The Kohn-Sham Formulation

The Kohn-Sham (KS) formulation [3] is of central importance to the application of density functional theory to quantum chemical problems [13]. The Kohn-Sham treatment of the complex many-electron problem posed by real systems is based on a simpler one-electron approach which is introduced by means of a reference system of non-interacting electrons which move under

the influence of a local external potential $v_{ref}(\mathbf{r})$.

The Hamiltonian for this reference system is a sum of one-electron Hamiltonians (due to the absence of electron-electron repulsion),

$$\hat{H}_{ref} = \sum_i \hat{h}_{ref}(i) = \sum_i \left[-\frac{1}{2}\nabla_i^2 + v_{ref}(\mathbf{r}_i) \right] \tag{2.31}$$

and the wavefunction is correctly represented by a Slater determinant. The fundamental connection between the non-interacting reference system and the real system of interacting electrons lies in the fact that both systems possess the same ground-state electron density, that is,

$$\rho_{ref} = \sum_i |\phi_i|^2 = \rho_{exact} \tag{2.32}$$

where the Kohn-Sham orbitals ϕ_i are the solutions to the one-electron equations associated with the reference system

$$\hat{h}_{ref}\, \phi_i \;=\; \epsilon_i\, \phi_i \tag{2.33}$$

From equations (2.25) and (2.27), the energy functional has the general form

$$E[\rho] = T_{el}[\rho] + V[\rho] + U_{ee}[\rho] \tag{2.34}$$

With the introduction of the reference system, equation (2.34) for the real interacting system can be recast as

$$E[\rho] = T_{ref}[\rho] + V[\rho] + J[\rho] + E_{xc}[\rho] \tag{2.35}$$

where $T_{ref}[\rho]$ is the kinetic energy of the reference system

$$T_{ref}[\rho] = \sum_i < \phi_i | -\frac{1}{2}\nabla_i^2 | \phi_i > \tag{2.36}$$

$V[\rho]$ is the external potential energy for the interacting system, $J[\rho]$ is the classical Coulomb potential energy, and $E_{xc}[\rho]$ is the exchange-correlation energy, given by

$$E_{xc}[\rho] = T[\rho] - T_{ref}[\rho] + U_{ee}[\rho] - J[\rho] \tag{2.37}$$

The Kohn-Sham equations for the real system are

$$\hat{h}_{eff}(i)\,\phi_i = \left[-\frac{1}{2}\nabla_i^2 + v_{eff}\right]\,\phi_i = \epsilon_i\,\phi_i \tag{2.38}$$

where the Kohn-Sham effective potential v_{eff} is

$$v_{eff}(\mathbf{r}) = v(\mathbf{r}) + \frac{\delta J[\rho]}{\delta \rho(\mathbf{r})} + \frac{\delta E_{xc}[\rho]}{\delta \rho(\mathbf{r})} \tag{2.39}$$

and

$$v_{xc}(\mathbf{r}) = \frac{\delta E_{xc}[\rho]}{\delta \rho(\mathbf{r})} \tag{2.40}$$

defines the exchange-correlation potential.

The total energy is given by equation (2.35) but it can also be expressed in terms of the Kohn-Sham orbital energies as [1]

$$E[\rho] = \sum_i \epsilon_i - \frac{1}{2}\int \frac{\rho(\mathbf{r})\rho(\mathbf{r}')}{|\mathbf{r}-\mathbf{r}'|}\, d\mathbf{r}\, d\mathbf{r}' + E_{xc}[\rho] - \int v_{xc}(\mathbf{r})\rho(\mathbf{r})\, d\mathbf{r} \qquad (2.41)$$

where

$$\sum_i \epsilon_i = T_{ref}[\rho] + \int v_{eff}(\mathbf{r})\rho(\mathbf{r})\, d\mathbf{r} \qquad (2.42)$$

Equations (2.41) and (2.42) show that the total electronic energy is not given by the sum of the orbital energies, just as in the Hartree-Fock method.

The significance of the Kohn-Sham approach has been clearly stated by Kohn, Becke, and Parr [11]: " ... in spite of the appearance of simple, single particle orbitals, the KS equations are in principle exact provided that the exact E_{xc} is used ... the only error in the theory is due to approximations of E_{xc} ".

2.2.2 Density Functionals

The fact that density functional theory is exact but the exact form of the energy functional is not known implies that approximate formulations of E_{xc} have to be employed in order for density functional calculations to be practicable. The development and testing of functionals is thus a central issue and a major challenge in modern DFT [9].

The solid foundations of density functional theory were established by the

Hohenberg and Kohn theorems, but long before this work, Thomas, Fermi, and Dirac had already developed models that focused on the electron density as the central variable in the description of electronic structure and behaviour [1].

The Thomas-Fermi (TF) energy functional is

$$E_{TF}[\rho] = C_F \int \rho(\mathbf{r})^{5/3}\, d\mathbf{r} + \int \rho(\mathbf{r}) v(\mathbf{r})\, d\mathbf{r} + J[\rho] \tag{2.43}$$

where the first term on the right-hand side represents the kinetic energy functional, taken from the theory of a non-interacting uniform electron gas [1, 4, 78], $J[\rho]$ replaces $U_{ee}[\rho]$ of equation (2.34) — thus, non-classical electron-electron interactions are neglected —, and $C_F = 2.8712$ [1].

The Thomas-Fermi-Dirac (TFD) energy functional extends the TF model by including the exchange-energy functional of a uniform electron gas

$$E_{TFD}[\rho] = E_{TF}[\rho] - C_x \int \rho(\mathbf{r})^{4/3}\, d\mathbf{r} \tag{2.44}$$

where $C_x = 0.7386$ [1].

The TF method is a rather crude model. In fact, its accuracy for atoms is rather limited, and its application to molecules has been completely unsuccessful since it fails to predict bonding [1]. Nevertheless, the TF model does contain " all the important ingredients of a density functional theory "[4] and is the first example of application of " one of the most important ideas in modern density functional theory, the local density approximation " [1].

The Local Density Approximation (LDA) [3] is the simplest expression for the energy functional of DFT. The exchange-correlation energy is given in the LDA by

$$E_{xc}^{LDA}(\rho) = \int \rho(\mathbf{r})\, \epsilon_{xc}(\rho)\, d\mathbf{r} \tag{2.45}$$

where $\epsilon_{xc}(\rho)$ is the exchange-correlation energy per particle of a uniform electron gas of density ρ [1, 4, 78]. Thus, the LDA applies locally the relations and results for a uniform electronic system to the description of systems which have inhomogeneous electron distributions, such as atoms, molecules, and solids. Although there is no formal justification for this procedure, many successful applications support the use of LDA in chemistry [7].

Separation of the exchange and correlation contributions is usual in DFT, so $\epsilon_{xc}(\rho)$ may be expressed as

$$\epsilon_{xc}(\rho) = \epsilon_x(\rho) + \epsilon_c(\rho) \tag{2.46}$$

where the exchange contribution is from Dirac's exchange functional of equation (2.44)

$$\epsilon_x(\rho) = -\frac{3}{4}\left(\frac{3}{\pi}\right)^{1/3} \rho(\mathbf{r})^{1/3} \tag{2.47}$$

Analytic forms for $\epsilon_c(\rho)$ have been derived [79–81] from the results of Monte Carlo calculations on the electron gas [82].

Ignoring the correlation contribution in equation (2.45) leads to Slater's $X\alpha$ method [83] which was developed before the work of Hohenberg, Kohn,

and Sham. A simplification of the Hartree-Fock method is achieved by replacing the complicated non-local Fock operator by a simpler local operator, named the $X\alpha$ local potential and defined by

$$v_{X\alpha}(\mathbf{r}) = -\frac{3}{2}\,\alpha\left[\frac{3}{\pi}\rho(\mathbf{r})\right]^{1/3} \tag{2.48}$$

In atomic and molecular electronic structure calculations, α has been used as an adjustable parameter, the best results having been obtained with $\alpha \sim 0.75$ [1].

A generalization of the LDA to treat α-spin and β-spin densities separately is the Local Spin Density (LSD) approximation [1, 84] in which

$$\rho(\mathbf{r}) = \rho^{\alpha}(\mathbf{r}) + \rho^{\beta}(\mathbf{r}) \tag{2.49}$$

and the exchange energy becomes

$$E_x^{LSD} = 2^{1/3} C_x \int [\rho^{\alpha}(\mathbf{r})^{4/3} + \rho^{\beta}(\mathbf{r})^{4/3}]\, d\mathbf{r} \tag{2.50}$$

The corresponding separation of correlation contributions is not possible because correlation effects, unlike exchange, involve both like-spin and unlike-spin interactions.

The LSD is needed for correctly describing systems under the influence of an external magnetic field, but it is also necessary (in the absence of a magnetic field) for the treatment of spin-polarized systems and relativistic effects. Furthermore, there is a more fundamental reason that favours LSD over LDA. Were the exact form of functionals known, LSD and LDA should

produce the same results where no net magnetic effects are present. However, for calculations on real systems approximate functional expressions must be introduced, and it turns out that the performance of approximate LSD functionals usually surpasses that of approximate LDA functionals [1, 84].

A systematic extension [78] of the LDA is obtained by means of gradient expansions of the form

$$E_x[\rho] = A_x \int \rho(\mathbf{r})^{4/3}\, d\mathbf{r} + B_x \int \frac{|\nabla\rho|^2}{\rho(\mathbf{r})^{4/3}}\, d\mathbf{r} + \cdots \tag{2.51}$$

where A_x and B_x are constants. Although Gradient Expansion Approximations (GEA) may appear to be the natural step for improving upon the LDA description, it has been found that they fail to yield quantitatively significant results [78].

The failure of the GEA led to the development of methods based on a different type of gradient-based corrections, the so-called Generalized Gradient Approximation (GGA) [11, 15, 78, 85]. In the GGA, the exchange-correlation energy is given by

$$E_{xc}^{GGA} = \int f(\rho^\alpha,\, \rho^\beta,\, \nabla\rho^\alpha,\, \nabla\rho^\beta)\, d\mathbf{r} \tag{2.52}$$

where f represents a function of the density and density gradients. Among the most popular GGA functionals are those developed by Perdew [87], Becke [88], Perdew and Wang [78, 86], and Lee, Yang, and Parr [89].

The LDA and LSD have been described as "remarkably useful structural, though not thermochemical, tools" [11]. With the development of the GGAs, DFT has also become a good approach to chemical energetics. However, the

GGA has not been clearly superior in applications of DFT to the study of properties of solid state systems [90].

The GGA functionals have certainly broadened the spectrum of chemical problems to which DFT can be reliably applied, but they still have deficiencies [11]. Extensive effort has been devoted to improving the GGA by incorporating some exactly computed exchange [91–94]. The resulting scheme (usually called hybrid methods) has proven remarkably successful in a wide variety of chemical applications [95, 96].

Approaches to the exchange-energy functional that go beyond the GGA are also being explored. Becke [97] has recently introduced second-order gradient corrections through a new inhomogeneity parameter q^σ. The new functional takes the general form

$$E_{xc} = \int f(\rho^\alpha, \rho^\beta, q^\alpha, q^\beta)\, d\mathbf{r} \tag{2.53}$$

where q^α and q^β depend on the density ρ and the first-order and second-order gradients, $\nabla\rho$ and $\nabla^2\rho$ [97].

For some particular systems, highly accurate conventional quantum chemical results are available. Therefore, there is interest in using these accurate electron densities to find highly accurate expressions for the exchange-correlation potential. High-quality information on a specific system can shed light on how to systematically upgrade the existing approximate functionals, and may eventually lead to the exact treatment of exchange and correlation [9, 13].

2.3 A Comparison between DFT and Traditional Methods

The fundamental conceptual difference between DFT and traditional quantum chemistry has been stated in the introduction to this chapter and some of the details have been discussed in the preceding sections.

Both the Hartree-Fock method and the Kohn-Sham method constitute one-electron approaches to the many-body electronic problem. Their basic formalism is indeed very similar, as revealed by inspection of the Hartree-Fock equations, (2.8) and (2.9), and of the Kohn-Sham equations, (2.38). However, the HF effective potential, equation (2.11), contains a (complicated) non-local exchange operator, equation (2.13), and lacks electron correlation effects. On the other hand, the exchange-correlation potential, equation (2.40), in the KS effective potential, equation (2.39), is a (simple) local operator that explicitly includes the effects of both electron exchange and correlation.

In traditional quantum chemistry, the HF approximation can be used as a starting point, and it can be improved upon by systematically incorporating increasingly accurate treatments of electron correlation effects via configuration interaction, many-body perturbation, or coupled-cluster techniques. Achieving high accuracy is, however, very costly since the computational dependence of post-HF methods on the molecular size M is of the order of M^5 – M^7 [16]. Accuracy in DFT lies in the expression for the exchange-correlation functional. The closer to the exact E_{xc}, the more accurate the results but there is no clear, systematic procedure that can be followed to bring approximate functionals closer to the exact E_{xc}. A major advantage of DFT is the fact that it can yield results that are as accurate as (and sometimes more accurate than) those obtained from more conventional ab initio

techniques, with considerably reduced computational demands [95]. In fact, density functional methods that depend linearly on the molecular size have already been developed [9].

A physical interpretation can be easily associated with the Hartree-Fock single-orbital energies by recourse to Koopmans' theorem (Section 2.1.1). On the other hand, the physical interpretation of the Kohn-Sham orbitals has been a rather controversial subject. It is clear that the energy of the highest occupied KS orbital is equal to the exact first ionization energy of the system, $\epsilon_{HOMO} = -IP^{\,exact}$ [13], but opinions have been varied regarding the general significance of the KS orbitals. Some examples are

Levine [98]: " The Kohn-Sham orbitals have no physical significance other than in allowing the exact ρ to be calculated ... the Kohn-Sham orbital energies should not be confused with molecular-orbital energies. "

Parr and Yang [1]: " Given the auxiliary nature of the KS orbitals — just N orbitals the sum of squares of which add up to the true total electron density — one should expect no simple physical meaning for the Kohn-Sham orbital energies. There is none. "

Kohn, Becke, Parr [11]: " The individual eigenfunctions and eigenvalues, ϕ_j and ϵ_j, of the KS equations have no strict physical significance ... At the same time, all ϵ_j and ϕ_j are of great semiquantitative value, much like the Hartree-Fock energies and wavefunctions, often more so, because they reflect also correlation effects, and are consistent with the exact physical density "

Baerends, Gritsenko, van Leeuwen [99]: " The theoretical status of the Kohn-Sham model has received comparatively little attention, as may be evident

from the frequently voiced opinion that the Kohn-Sham orbitals are just a means to generate electron densities but do not have any physical meaning themselves. However, this is a far too restricted view on the Kohn-Sham model ... The Kohn-Sham orbitals represent electrons that move in a potential that is certainly as realistic as the Hartree-Fock 'potential' and indeed has some advantages. There is no reason to believe that the Kohn-Sham orbitals are any less 'physical' or useful than the Hartree-Fock orbitals ".

2.4 Computational Aspects of Quantum Chemical Methods

Practical strategies are essential to make the computation of electronic structure feasible. Numerical methods are common for atomic systems, but the majority of molecular calculations are performed using basis-set expansion methodology [4, 70, 73].

A finite set of appropriate basis functions $\{g_i\}$ is introduced and the spatial function of the molecular spin-orbitals is expressed as a linear combinations of these basis functions, that is

$$\varphi_k = \sum_i g_i C_{ik} \tag{2.54}$$

where the C_{ik} are expansion coefficients determined in the calculation process. The introduction of the basis set transforms the problem of solving the molecular electronic structure equations into a matrix eigenvalue problem [73, 100]. In the Hartree-Fock method, this matrix eigenvalue problem takes the form [73]

$$\mathbf{FC} = \mathbf{SC}\epsilon \tag{2.55}$$

The equivalent expression in the Kohn-Sham method is [100]

$$\mathbf{H}^{KS}\mathbf{C} = \mathbf{SC}\epsilon \tag{2.56}$$

In equations (2.55) and (2.56), $\mathbf{C}$ is the matrix of the coefficients C_{ik}, the orbital energies ϵ_i are the elements of the matrix ϵ, and the elements of the matrix $\mathbf{S}$ are the overlap integrals (the basis functions are usually non-orthogonal)

$$S_{ij} = \int g_i \, g_j \, d\mathbf{r} \tag{2.57}$$

The Fock matrix elements are given by

$$F_{ij} = \int g_i \, \hat{f} \, g_j \, d\mathbf{r} \tag{2.58}$$

and the corresponding Kohn-Sham matrix elements are

$$H_{ij}^{KS} = \int g_i \, \hat{h}_{eff} \, g_j \, d\mathbf{r} \tag{2.59}$$

Both the HF and the KS equations depend on the orbitals which are the solutions to the equations. This apparent dilemma is solved by means of a self-consistent field (SCF) approach. The calculations are started with a reasonable guess for the orbitals and the equations are solved in an iterative

fashion. The computational procedure is stopped when a given convergence criterion is met (for example, the total energy difference between two consecutive cycles has to remain smaller than a specified value for a certain number of iterations), at which point the solutions are said to be self-consistent.

2.4.1 Basis Sets

The most widely used basis functions for molecular electronic structure calculations are Slater-type orbitals (STO) and Gaussian-type orbitals (GTO) [4, 70, 73]. The general form of an STO is

$$g_{STO}(\mathbf{r}) = C_N r^{n-1} e^{-\zeta \mathbf{r}} Y_{lm}(\theta, \phi) \tag{2.60}$$

Cartesian GTOs are defined by

$$g_{GTO}(\mathbf{r}) = C_N x^a y^b z^c e^{-\zeta r^2} \tag{2.61}$$

In equations (2.60) and (2.61) C_N is a normalization constant, $Y_{lm}(\theta, \phi)$ is a spherical harmonic [70], and ζ is a positive exponent. The sum of the non-negative integers a, b, and c defines the type of Cartesian Gaussian: an s-type Gaussian has $a + b + c = 0$, a p-type Gaussian has $a + b + c = 1$, a d-type Gaussian has $a + b + c = 2$, and so on. Spherical Gaussians — which include spherical harmonics — can also be used.

STOs provide a better representation of the electronic wavefunctions near the nucleus of an atom, but they render the evaluation of electron integrals complicated. On the other hand, the mathematical form of a GTO is con-

venient for computational purposes. GTOs are then usually preferred, especially for calculations on relatively large systems.

There is however a disadvantage in using GTOs in that they are functions of inferior quality when compared with STOs. Therefore, a larger number of GTOs are necessary to obtain results of the same accuracy as that achieved by STO basis sets. A practical solution to this problem which permits to take advantage of the computational convenience of GTOs is the use of basis sets consisting of contracted Gaussians. A contracted Gaussian function is a fixed linear combination of primitive Gaussian functions, and can be constructed through a least-square fit of primitive Gaussians to STOs which have been already optimized in an atomic calculation [70, 73].

In molecular calculations the choice of basis sets is a compromise between accuracy (which demands large basis sets) and computational requirements (which favour smaller basis sets). A minimal basis set is the simplest form as only one basis function is used to represent each orbital, but it is seldom capable of yielding accurate results. In order to improve upon the minimal basis set performance, the set is extended by including twice, three times, four times, five times, and so on, as many functions as there are orbitals thus generating the so-called double-zeta, triple-zeta, quadruple-zeta, quintuple-zeta, and so on, basis sets. Incorporation of functions of higher angular momentum quantum number [70] than that of the valence electrons is also important. These functions are called polarization functions because they are required for the description of the polarization of an atom in a molecular field.

Chapter 3

Computational Approach

In this chapter, the general methodology involved in the calculation of the core-electron binding energies reported in Chapters 4, 5, and 6 will be described. The formalism associated with the unrestricted generalized transition state (uGTS) model and the ΔE-KS approach will be presented first, followed by a description of some of the details of the density functional program and the basis sets employed for the computation of the CEBEs.

3.1 The uGTS and ΔE-KS Approaches

The energetics of an electron removal process, such as the ionization from a core level, can be generically represented as the difference in the total energy of the initial and final states of the electronic system

$$\Delta E = E_{final} - E_{initial} \tag{3.1}$$

The total energy can be expressed as an analytic function of the occupation numbers n_i of a set of one-electron molecular orbitals ϕ_i [62], that is

$$E = E(n_1, n_2, n_3, \ldots, n_N) \tag{3.2}$$

and the electron density of the electronic system is defined by

$$\rho = \sum_i n_i |\phi_i|^2 \tag{3.3}$$

Equation (3.3) is a generalization of (2.32) and allows for fractional occupation of the molecular orbitals [1]. From (3.1) and (3.2), a core-ionization energy is given by

$$\Delta E = E(0, 1, 1, \ldots, 1) - E(1, 1, 1, \ldots, 1) \tag{3.4}$$

The calculation of core-electron binding energies according to equation (3.4) using Kohn-Sham DFT constitutes the ΔE-KS approach. The results of the application of this method to the determination of molecular CEBEs will be presented in Chapters 5 and 6.

Slater's transition state (TS) [62] model and its generalization by Williams, deGroot, and Sommers [69] are approximations to equation (3.4). If the total energy is represented as a function of a continuous variable λ (which can be related to orbital occupation) by the series expansion [18]

$$E(\lambda) = E_0 + \lambda E_1 + \lambda^2 E_2 + \lambda^3 E_3 + \lambda^4 E_4 + \lambda^5 E_5 + \cdots \tag{3.5}$$

then equation (3.4) becomes

$$\Delta E = E(1) - E(0) = E_1 + E_2 + E_3 + E_4 + E_5 + \cdots \tag{3.6}$$

where $E(0)$ and $E(1)$ give the energies of the initial and final states, respectively. In DFT, according to Janak's theorem [101], the first derivative of the total energy with respect to the occupation number of an orbital is equal to the energy of that orbital, that is

$$\frac{\partial E}{\partial n_i} = \epsilon_i \tag{3.7}$$

For the ionization of an electron from the ith molecular orbital ϕ_i, λ represents the fraction of an electron removed. Therefore, application of Janak's theorem leads to

$$\frac{\partial E}{\partial \lambda} = -\epsilon_i \tag{3.8}$$

From equation (3.5), the first derivative is given by

$$\frac{\partial E}{\partial \lambda} = F(\lambda) = E_1 + 2\lambda E_2 + 3\lambda^2 E_3 + 4\lambda^3 E_4 + 5\lambda^4 E_5 + \cdots \tag{3.9}$$

Slater's TS model uses $\lambda = \frac{1}{2}$ to approximate ΔE as

$$F\left(\frac{1}{2}\right) = E_1 + E_2 + \frac{3}{4}E_3 + \frac{1}{2}E_4 + \frac{5}{16}E_5 + \cdots \tag{3.10}$$

Therefore, the error of the TS model is

$$\delta_{TS} = -\frac{1}{4}E_3 - \frac{1}{2}E_4 - \frac{11}{16}E_5 + \cdots \tag{3.11}$$

In the generalized transition state (GTS) model, ΔE is calculated by

$$\Delta E = \frac{1}{4}\,F(0) + \frac{3}{4}\,F\left(\frac{2}{3}\right) \tag{3.12}$$

Thus, ΔE is approximated as

$$\Delta E = E_1 + E_2 + E_3 + \frac{8}{9}E_4 + \frac{80}{81}E_5 + \cdots \tag{3.13}$$

with an error

$$\delta_{GTS} = -\frac{1}{9}E_4 - \frac{7}{27}E_5 + \cdots \tag{3.14}$$

Calculations using the TS and GTS models can be performed in a restricted or an unrestricted fashion. In the former, $\frac{1}{4}$ spin-α electron and $\frac{1}{4}$ spin-β electron (TS) or $\frac{1}{3}$ spin-α electron and $\frac{1}{3}$ spin-β electron (GTS) are removed, whereas in the latter $\frac{1}{2}$ spin-α/β electron (TS) or $\frac{2}{3}$ spin-α/β electron (GTS) are removed. A study by Chong [18] showed that the uGTS approach gives the best results in density functional determinations of molecular CEBEs. Chapter 4 of this thesis contains the results of a number of applications of the uGTS model.

3.2 The Density Functional Program deMon

All the density functional calculations reported in this thesis were performed with the program deMon [102–104], which makes use of Gaussian-based density functional methodology in the form of Gaussian orbital and auxiliary basis sets.

The molecular orbitals are expanded in the orbital basis set as in equation (2.54), whereas both the density and the exchange-correlation potential are expanded in the auxiliary basis sets, that is

$$\tilde{\rho} = \sum_i a_i g_i^{\rho} \tag{3.15}$$

$$\tilde{V}_{xc} = \sum_i b_i g_i^{xc} \tag{3.16}$$

where $\tilde{\rho}$ and $\tilde{V}_{xc}$ are fits to ρ and V_{xc}, respectively.

The density fitting coefficients a_i are obtained analytically via a least squares fitting procedure by requiring that the error in the Coulomb energy

$$\int\int [\rho(\mathbf{r}_1) - \tilde{\rho}(\mathbf{r}_1)] \frac{1}{r_{12}} [\rho(\mathbf{r}_2) - \tilde{\rho}(\mathbf{r}_2)] \, d\mathbf{r}_1 \, d\mathbf{r}_2 \tag{3.17}$$

be minimized and the fitted density $\tilde{\rho}$ be normalized to the total number of electrons.

The potential fitting coefficients b_i are determined by performing a least squares fit over a set of grid points centered about each atom. This procedure minimizes the error in the fitted potentials over the sum of the grid points.

By representing the density and the exchange-correlation potential as linear combinations of Gaussian functions, the integrals in which ρ and V_{xc} are involved are given a simpler mathematical form and the computational demands are alleviated. In fact, if n_O is the number of orbital basis functions and n_A is the number of auxiliary basis functions, the computational effort in GTO-based DFT scales formally as $(n_O)^2\, n_A$, compared with $(n_O)^4$ for Hartree-Fock methods and at least $(n_O)^5$ for conventional correlated methods.

3.2.1 Basis Sets

In deMon, the Gaussian functions used are *s*-, *p*-, and *d*-type GTOs (orbitals of higher angular momentum quantum number such as *f*-type functions cannot be included).

The auxiliary basis sets are described by the general notation $(j, k; m, n)$, where j and k are, respectively, the number of *s*-type GTOs and the number of sets of *s*-, *p*-, and *d*-type GTOs for the density fit, and m and n are the corresponding number of basis functions and number of sets for the exchange-correlation potential fit.

The auxiliary fitting functions denoted by (3,1;3,1) for hydrogen, (4,4;4,4) for boron, carbon, nitrogen, oxygen, and fluorine, (5,4;5,4) for silicon, phosphorus, sulphur, chlorine, and argon, and (5,5;5,5) for chromium, vanadium, germanium, bromine, and iodine were employed in the calculations.

The orbital basis sets used were the *s*, *p*, *d* parts of the correlation-consistent polarized valence basis set given by Dunning and coworkers [105,

106]. These sets are described by the general notation cc-pVnZ, where n indicates the quality of the basis functions: T for triple-zeta, Q for quadruple-zeta, and 5 for quintuple-zeta. The cc-pVnZ basis sets were used for hydrogen, the second-period elements boron through fluorine, and the third-period elements silicon through argon. The basis sets of double-zeta quality denoted by DZVP or DZVP2 [107] — which are included in deMon — were employed for chromium, vanadium, germanium, bromine, and iodine.

For hydrogen, cc-pVnZ basis sets consisted of n sets of s-type functions and p-type functions were used as polarization functions. For second- and third-period elements, the composition of the basis sets was as given in Table 3-1. The d-type basis functions consisted of six cartesian components.

Table 3-1. Composition of cc-pVnZ basis sets.

basis set	number of functions		
	s-type	**p-type**	**d-type**
	second-period elements		
cc-pVTZ	4	3	2
cc-pVQZ	5	4	3
cc-pV5Z	6	5	4
	third-period elements		
cc-pVTZ	5	4	2
cc-pVQZ	6	5	3
cc-pV5Z	7	6	4

The initial investigations carried out by Chong [18, 19] showed that uGTS/DFT calculations of CEBEs using the cc-pV5Z basis set were in excellent agreement with experimental results. Nevertheless, application of this approach to relatively large molecules — and eventually to species large enough to be realistic models for extended systems — becomes prohibitively expensive as far as computational demands are concerned. A viable alternative is to use smaller basis sets modified to improve the description of the core-hole state involved in CEBE calculations. Chong and coworkers [20] proposed a modification of the cc-pVTZ basis set based on an exponent scaling factor designed to provide a more efficient representation of the shielding effects associated with the partially ionized state. The scaled basis sets were thoroughly tested on a variety of molecules [20, 24, 25, 29] — including relatively large transition metal carbonyls and nitrosyls [22] — with remarkably good results. In fact, the performance of the scaled-pVTZ basis set was almost as good as that of the much larger cc-pV5Z set.

For GTO basis functions, the scaling factor for the exponent is the square of the ratio of the effective nuclear charge

$$scaling = \left(\frac{Z - \sigma'}{Z - \sigma}\right)^2 \tag{3.18}$$

where Z is the nuclear charge of the atom considered, σ and σ' are the screening constants of the neutral molecule and the (partially) core-ionized cation, respectively. The screening constants were determined using the formulas provided by Clementi and Raimondi [108]. For boron through neon, they are given by

$$\sigma(1s) = 0.3 + 0.0072(Z - 2) \tag{3.19}$$

$$\sigma(2s) = 1.7208 + 0.3601(Z - 3) \tag{3.20}$$

$$\sigma(2p) = 2.5787 + 0.3326(Z - 5) \tag{3.21}$$

In the uGTS approach, the modified screening constants (due to the removal of two thirds of an electron from a core $1s$ orbital) were calculated via

$$\sigma'(1s) = \left(\frac{1}{3}\right)\ 0.3 + 0.0072(Z - 2) \tag{3.22}$$

$$\sigma'(2s) = \left(\frac{2}{3}\right)\ 1.7208 + 0.3601(Z - 3) \tag{3.23}$$

$$\sigma'(2p) = \left(\frac{2}{3}\right)\ 1.8585 + 0.7202 + 0.3326(Z - 5) \tag{3.24}$$

In equation (3.24) the screening factor 2.5787 was arbitrarily partitioned into 1.8585 and 0.7202 in order to consider $1s$ electron and $2s$ electron effects separately. An equivalent partition into 1.7208 ($1s$) and 0.8579 ($2s$) had negligible effects [20]. The scaling factors determined from equation (3.18) [20] are shown in Table 3-2. Results of calculations performed with scaled-pVTZ and scaled-pVQZ basis sets will be presented in Chapter 4.

Table 3-2. Scaling factors (uGTS) for second-period atoms.

atom	1s	2s	2p
B	1.0873268	1.4985434	1.5771700
C	1.0717755	1.3907759	1.4413679
N	1.0609247	1.3211702	1.3570659
O	1.0529234	1.2725484	1.2997082
F	1.0467796	1.2366817	1.2581833

Scaled basis sets were also employed within the ΔE-KS approach. In this case, screening constants for a fully ionized cation are needed. For $1s$ and $2s$ orbitals, they were calculated by

$$\sigma'(1s) = 0.0072(Z-2) \tag{3.25}$$

$$\sigma'(2s) = \left(\frac{1}{2}\right)\ 1.7208 + 0.3601(Z-3) \tag{3.26}$$

Three different $2p$ scaling factors were obtained and tested. The screening constants were determined using different partition schemes as follows

$$\sigma'_I(2p) = \left(\frac{1}{2}\right)\ 1.8585 + 0.7202 + 0.3326(Z-5) \tag{3.27}$$

$$\sigma'_{II}(2p) = \left(\frac{1}{2}\right) \; 1.7208 + 0.8579 + 0.3326(Z-5) \tag{3.28}$$

$$\sigma'_{III}(2p) = \left(\frac{3}{4}\right) \; 2.5787 + 0.3326(Z-5) \tag{3.29}$$

The corresponding scaling factors from equation (3.18) are given in Table 3-3.

Table 3-3. Scaling factors (ΔE-KS) for second-period atoms.

atom	1s	2s	2p(I)	2p(II)	2p(III)
B	1.1323609	1.7854975	1.9147939	1.8369636	1.6034193
C	1.1085960	1.6102784	1.6922230	1.6347254	1.4610248
N	1.0920626	1.4985005	1.5560007	1.5106066	1.3727422
O	1.0798969	1.4211246	1.4642723	1.4268460	1.3127300
F	1.0705703	1.3644409	1.3983809	1.3665784	1.2693126

Another type of basis set, labeled as cc-pCVTZ [109], was also tested in ΔE-KS calculations. It represents an extension of the cc-pVTZ set developed to treat core and core-valence correlation effects more efficiently. The new basis set of triple-zeta quality adds two *s*-type, two *p*-type, and one *d*-type functions to the original set. Therefore, the number of basis functions grows

from [4s3p2d] (Table 3-1) for cc-pVTZ to [6s5p3d] for cc-pCVTZ, but the latter is still smaller than a cc-pV5Z set, and it is a legitimate option for the treatment of fairly large systems. The results of the ΔE-KS calculations with scaled-pVTZ and cc-pCVTZ sets will be discussed in Chapter 6.

Chapter 4

Applications of the uGTS Model

The results of calculations of core-electron binding energies using the unrestricted generalized transition state approach described in Section 3.1 are contained in this chapter. Extensive calculations by Chong and coworkers [18-25] have already demonstrated that the uGTS/DFT approach yields C, N, O, and F CEBEs in very good agreement with experiment. Thus, the investigations reported in this chapter represent an extension of this approach to boron-containing molecules, to some additional isomer cases, and to the third-period elements Si, P, S, Cl, and Ar.

All calculations were performed using experimental geometries [110] of the neutral parent molecules and the functional labeled B88/P86, which consists of Becke's 1988 exchange functional [88] and Perdew's 1986 correlation functional [87]. The B88/P86 combination and some other functional choices available in deMon were tested by Chong [18]. The results obtained showed

that the B88/P86 functional delivers the best performance in uGTS-based calculations of CEBEs.

Relativistic effects must be taken into account when calculating large binding energies such as those of core-level electrons because the velocity of an electron in an atom's inner shell is not negligible compared to the velocity of light [33]. The results of the calculations for second-period elements were modified with approximate relativistic corrections, based on the studies by Pekeris [111] for two-electron ions. The corrections were estimated with the following empirically derived equation [19]

$$C_{rel} = A\, I_{nrel}^{B} \tag{4.1}$$

where C_{rel} is the relativistic correction, I_{nrel} is the non-relativistic CEBE in eV, $A = 2.198 \cdot 10^{-7}$, and $B = 2.178$. A and B are two fitting parameters of the relation between the relativistic correction and the non-relativistic CEBEs for Pekeris' two-electron ions. Relativistic corrections for core-ionization energies of third-period elements were not available.

4.1 Boron-Containing Molecules

The results for boron CEBEs are summarized in Tables 4-1 and 4-2. The range of experimental CEBEs [40, 112] is almost 10 eV, from 192.9 eV for $BH_3P(CH_3)_3$ to 202.8 eV for BF_3. The CEBEs of C, N, O, and F were also calculated and are shown in Tables 4-3 and 4-4.

Table 4-1. Basis set convergence in the calculation of B 1s energies (in eV) with unscaled basis sets. Calculated CEBEs include relativistic corrections from equation (4.1).

molecule	cc-pVTZ	cc-pVQZ	cc-pV5Z	experiment
BF_3	202.44	202.21	202.17	202.80
BCl_3	199.83	199.50	199.45	199.80
BBr_3	199.19	198.84	198.80	199.00
BI_3	198.25	197.86	197.80	197.80
B_2H_6	196.84	196.59	196.56	196.50
BH_3CO	195.59	195.34	195.31	195.15
BH_3PF_3	195.16	194.84	194.79	194.69
BH_3NH_3	194.46	194.17	194.14	193.73
BH_3CNCH_3	194.07	193.82	193.78	193.60
BF_3PH_3	199.54	199.31	199.28	

Average absolute deviations (AAD) and maximum deviations (MD) of the calculated CEBEs from the experimental values and from the estimated complete basis set (CBS) limits are given in Table 4-5. The estimated CBS limits for 19 of the test cases were determined from the results of the corresponding cc-pVTZ, cc-pVQZ, and cc-pV5Z calculations, according to the empirically derived equation [113]

$$A(x) = A(\infty) + B\,e^{-Cx} \tag{4.2}$$

where x is the cardinal number of the basis set (3, 4, 5 for TZ, QZ, 5Z, respectively) and $A(\infty)$ is the estimated CBS limit for the property.

Table 4-2. Calculations of B core-electron binding energies (in eV) with scaled basis sets. Calculated CEBEs include relativistic corrections from equation (4.1).

molecule	scaled-pVTZ	scaled-pVQZ	experiment
$\mathbf{B}F_3$	202.23	202.19	202.80
$\mathbf{B}Cl_3$	199.54	199.50	199.80
$\mathbf{B}Br_3$	198.86	198.83	199.00
$\mathbf{B}I_3$	197.89	197.84	197.80
$\mathbf{B}H_3CO$	195.37	195.33	195.15
$\mathbf{B}H_3PF_3$	194.90	194.83	194.69
$\mathbf{B}H_3NH_3$	194.20	194.16	193.73
$\mathbf{B}H_3CNCH_3$	193.85	193.81	193.60
$\mathbf{B}H_3N(CH_3)_3$	193.57		193.37
$\mathbf{B}H_3P(CH_3)_3$	193.00		192.93
$\mathbf{B}_2H_6$	196.63	196.58	196.50
$\mathbf{B}_5H_9$ – *base*	196.27		196.10
$\mathbf{B}_5H_9$ – *apex*	194.26		194.20
$1,5-\mathbf{B}_3C_2H_5$	196.28		196.00
$1,6-\mathbf{B}_4C_2H_6$	195.67		195.40
$\mathbf{B}(OCH_3)_3$	197.52		197.80
$\mathbf{B}(CH_3)_3$	195.91		196.40
$\mathbf{B}F_3PH_3$	199.30	199.28	
$\mathbf{B}_3N_3H_6$	196.08		

Table 4-3. Basis set convergence in the calculation of C, N, O, and F 1s energies (in eV) with unscaled basis sets. Calculated CEBEs include relativistic corrections from equation (4.1).

molecule	cc-pVTZ	cc-pVQZ	cc-pV5Z	experiment
BH_3 **C** O	296.03	295.74	295.70	296.18
BH_3CN **C** H_3	294.21	293.91	293.87	294.06
BH_3 **C** NCH_3	293.36	293.12	293.07	293.43
BH_3 **N** H_3	408.64	408.25	408.20	408.41
BH_3C **N** CH_3	407.43	407.08	407.03	407.13
BH_3C **O**	542.29	541.87	541.80	542.05
B **F** $_3$	695.24	694.72	694.65	694.80
BH_3P **F** $_3$	695.41	694.89	694.82	694.30
B **F** $_3PH_3$	692.58	692.10	692.03	

For the 9 cases studied with the cc-pVQZ and cc-pV5Z basis sets and the 17 cases investigated with the cc-pVTZ basis set, the AAD from experiment for the boron CEBEs was smallest for cc-pV5Z, and the cc-pVQZ performance was almost as good as that of cc-pV5Z. It is also observed that with exponent scaling the results from the triple-zeta basis set (scaled-pVTZ) significantly improved upon those from the corresponding unscaled basis set (cc-pVTZ), and they were brought much closer to the results obtained from cc-pV5Z calculations. Exponent scaling did not have an appreciable effect on the performance of the pVQZ basis set as far as agreement with experimental

Table 4-4. Calculations of C, N, O, and F core-electron binding energies (in eV) with scaled basis sets. Calculated CEBEs include relativistic corrections from equation (4.1).

molecule	scaled-pVTZ	scaled-pVQZ	experiment
$BH_3\,\mathbf{C}\,O$	295.74	295.72	296.18
$BH_3CN\,\mathbf{C}\,H_3$	293.93	293.90	294.06
$BH_3\,\mathbf{C}\,NCH_3$	293.12	293.10	293.43
$B(O\,\mathbf{C}\,H_3)_3$	292.36		292.20
$BH_3N(\,\mathbf{C}\,H_3)_3$	292.27		291.97
$1,6-B_4\,\mathbf{C}_2H_6$	291.59		291.30
$BH_3P(\,\mathbf{C}\,H_3)_3$	291.28		290.96
$1,5-B_3\,\mathbf{C}_2H_5$	290.52		290.20
$BH_3\,\mathbf{N}\,H_3$	408.28	408.23	408.41
$BH_3C\,\mathbf{N}\,CH_3$	407.08	407.05	407.13
$BH_3\,\mathbf{N}\,(CH_3)_3$	407.23		406.68
$BH_3C\,\mathbf{O}$	541.86	541.83	542.05
$B(\,\mathbf{O}\,CH_3)_3$	538.49		538.30
$B\,\mathbf{F}_3$	694.71	694.69	694.80
$BH_3P\,\mathbf{F}_3$	694.88	694.85	694.30
$B\,\mathbf{F}_3PH_3$	692.03	692.06	
$B_3\,\mathbf{N}_3H_6$	405.01		

results is concerned. However, comparisons with the estimated CBS limits are more meaningful if the aim is to design an efficient basis set applicable

Table 4-5. Average Absolute Deviation (in eV) and Maximum Deviation (in eV) of calculated core-electron binding energies from experiment and from CBS. The number of test cases is given in parentheses.

basis set	deviations from experiment		deviations from CBS	
	AAD	**MD**	**AAD**	**MD**
		boron test cases		
cc-pVTZ	0.36 (17)	+ 0.73	0.34 (10)	0.46
cc-pVQZ	0.24 (9)	− 0.59	0.05 (10)	0.07
cc-pV5Z	0.23 (9)	− 0.63	0.01 (10)	0.01
scaled-pVTZ	0.24 (17)	− 0.57	0.07 (10)	0.10
scaled-pVQZ	0.24 (9)	− 0.64	0.03 (10)	0.06
CBS	0.23 (9)	− 0.64		
		all test cases		
cc-pVTZ	0.41 (32)	+ 1.11	0.38 (19)	0.60
cc-pVQZ	0.25 (17)	± 0.59	0.06 (19)	0.08
cc-pV5Z	0.26 (17)	− 0.63	0.01 (19)	0.01
scaled-pVTZ	0.26 (32)	+ 0.58	0.07 (19)	0.10
scaled-pVQZ	0.24 (17)	− 0.61	0.04 (19)	0.06
CBS	0.26 (17)	− 0.64		

to large molecules. Also, experimental observations are affected by experimental error whereas the CBS limit gives a fixed value. Table 4-5 shows that the cc-pV5Z basis set approximated the CBS limit very well and that

the scaled-pVTZ basis set also performed satisfactorily. In the case of the scaled-pVQZ basis set, results do show some improvement upon those from cc-pVQZ calculations when compared with the CBS limit.

The effect of relativistic corrections is either very small or negligible for boron CEBEs. This was expected from the fact that the relativistic correction calculated via equation (4.1) was found to be only 0.02 eV for the boron 1s energies.

The results for the CEBEs of all five second-period elements investigated — 32 cases with pVTZ and 17 cases with pVQZ and pV5Z — gave an AAD from experiment of 0.26 eV for both the cc-pV5Z and scaled-pVTZ basis sets. This compares well with a previous study [24] of 66 CEBEs of small closed-shell molecules, in which the AAD was found to be 0.22 eV.

In the calculations with scaled basis sets, only the atom with the core hole is treated differently by making use of exponent scaling. Equations (3.19) through (3.21) can be rewritten as

$$\sigma(1s) = 0.3 + 0.0072(n_{2s} + n_{2p}) \tag{4.3}$$

$$\sigma(2s) = 1.7208 + 0.3601(n_{2s} + n_{2p} - 1) \tag{4.4}$$

$$\sigma(2p) = 2.5787 + 0.3326(n_{2p} - 1) \tag{4.5}$$

where n_{2s} and n_{2p} can be obtained from population analysis [73], and a general-scaled basis set can be constructed by calculating new screening constants from equations (4.3) through (4.5) and the corresponding scaling fac-

tors from equation (3.18), for each of the atoms in a given molecule. The resulting basis set was labeled gs-pVTZ when obtained from the cc-pVTZ set, and was tested in calculations of CEBEs for 12 of the test cases reported in this section. The results are given in Table 4-6, where they are compared with those from scaled-pVTZ basis sets. Table 4-7 presents an AAD-based analysis of the performance of the gs-pVTZ basis set.

Table 4-6. Calculations of core-electron binding energies (in eV) with the gs-pVTZ basis set. CEBEs include relativistic corrections from equation (4.1).

molecule	scaled-pVTZ	gs-pVTZ
$\mathbf{B}F_3$	202.23	202.22
$\mathbf{B}_2H_6$	196.63	196.60
$\mathbf{B}H_3CO$	195.37	195.33
$\mathbf{B}H_3NH_3$	194.20	194.15
$\mathbf{B}H_3CNCH_3$	193.85	193.81
$BH_3\,\mathbf{C}O$	295.74	295.74
$BH_3CN\,\mathbf{C}H_3$	293.93	293.92
$BH_3\,\mathbf{C}NCH_3$	293.12	293.11
$BH_3\,\mathbf{N}H_3$	408.28	408.25
$BH_3C\,\mathbf{N}CH_3$	407.08	407.07
$BH_3C\,\mathbf{O}$	541.86	541.84
$BH_3P\,\mathbf{F}_3$	694.71	694.67

Table 4-7. Deviation analysis (in eV) of the gs-pVTZ basis set performance for the 12 cases reported in Table 4-6.

basis set	deviations from experiment	deviations from CBS
	AAD	**AAD**
scaled-pVTZ	0.25	0.07
gs-pVTZ	0.25	0.04
cc-pV5Z	0.27	0.01

Although the use of generalized scaling helped to improve upon the performance of the single-atom scaling approach for the 12 cases investigated (this is reflected by the AAD from CBS), the gain is relatively small and is not justified by the large amount of additional effort that is required for obtaining the scaling factors and gs-pVTZ basis sets for all the atoms.

4.2 Isomers of C_3H_5NO

The total energies, relative energies with respect to the most stable isomer (ethyl isocyanate), and dipole moments of four isomers of C_3H_5NO are summarized in Table 4-8. Figure 4-1 shows the structures and atom numbering schemes for the isomers. For the three species with lowest energies (ethyl isocyanate, 2-azetidinone, 3-hydroxypropanenitrile) it is observed that the calculated dipole moments compare very well with the corresponding experimental values [114].

Table 4-8. Total energies (in eV), relative energies (in eV) with respect to ethyl isocyanate, and dipole moments (in D) for the isomers of C_3H_5NO.

isomer	**E**	**ΔE**	μ_{cal}	μ_{obs} [a]
ethyl isocyanate	-6732.0304	(0.0)	2.848	2.81±0.02
2-azetidinone	-6731.5353	0.4951	3.783	3.828
3-hydroxypropanenitrile	-6731.2750	0.7554	3.122	3.166
lactonitrile B	-6731.2302	0.8002	3.139	
lactonitrile A	-6731.1962	0.8342	2.982	

[a] reference 114

Two conformers have been reported [115] for the fourth isomer, lactonitrile. They were labeled A and B by the authors. Their microwave spectroscopic measurements indicated that conformer A was more stable than conformer B. DFT calculations were performed for both conformers using the experimental geometries reported by the authors, but the results did not agree with those from the microwave experiment, the total energy of conformer B having been found to be lower than that of conformer A. In addition, geometry optimizations were carried out (with the semiempirical method Austin Model 1, or AM1, [116] available in the software package called WinMOPAC Version 2 [117]) with both conformer A and B structures as starting geometries, and in both cases the calculations converged to the geometry of conformer B.

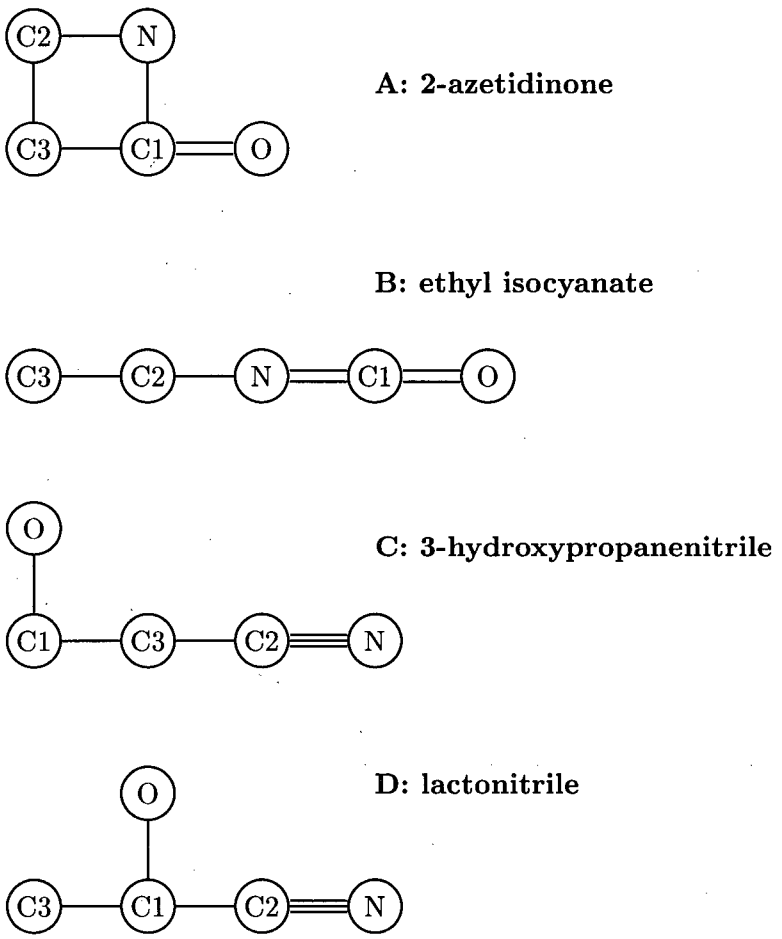

Figure 4-1. Numbering scheme for the isomers of C_3H_5NO. Hydrogen atoms are not shown.

Table 4-9 summarizes the CEBEs of the C_3H_5NO isomers. They are also shown schematically in Figure 4-2. Only the CEBEs of 2-azetidinone have been determined experimentally [41], and in this case the agreement between

Table 4-9. Core-electron binding energies (in eV) for the isomers of C_3H_5NO. Calculated CEBEs include relativistic corrections from equation (4.1)

isomer	atom	CEBE	experiment	deviation
2-azetidinone	O	537.35	537.32	+0.03
	N	405.95	405.76	+0.19
	C1	293.77		
	C2	292.43		
	C3	291.41		
ethyl isocyanate	O	539.44		
	N	405.96		
	C1	294.60		
	C2	292.59		
	C3	291.28		
3-hydroxypropanenitrile	O	539.41		
	N	405.71		
	C3	293.11		
	C1	292.85		
	C2	292.70		
lactonitrile B	O	539.57		
	N	405.67		
	C2	294.09		
	C1	292.70		
	C3	291.67		
lactonitrile A	O	539.60		
	N	405.65		
	C2	294.05		
	C1	292.67		
	C3	291.65		

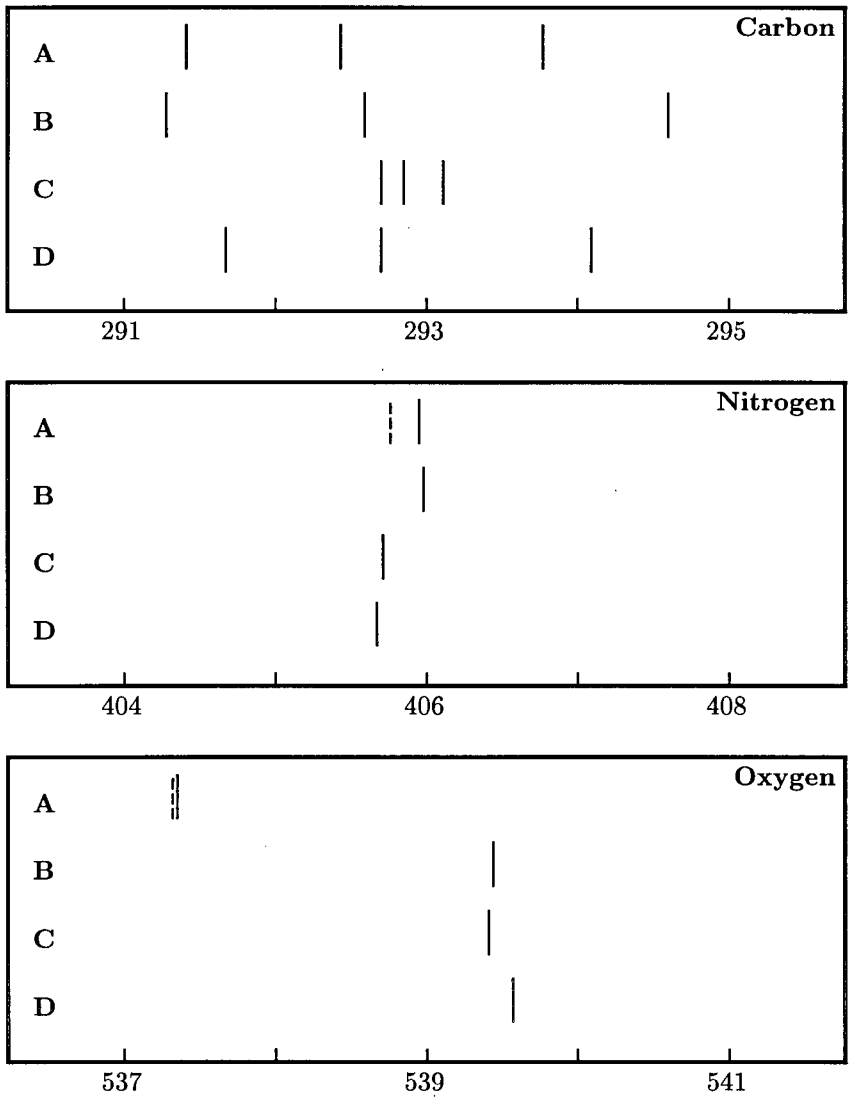

Figure 4-2. Calculated (solid lines) and available experimental (dashed lines) CEBEs for the isomers of C_3H_5NO.

calculated and observed energies is very good. All isomers possess a distinctive core-ionization spectrum, a demonstration of the analytical potential of ESCA. For 2-azetidinone, ethyl isocyanate, and lactonitrile, three clearly distinct C 1s energies are observed. In the case of 3-hydroxypropanenitrile, the C 1s energies are still different but much closer to one another. The N 1s energies are all similar, as are the O 1s energies, except for the CEBE value of 2-azetidinone which is considerably lower — about 2 eV — than those of the other three species. It should be noted that, with the increasing availability of high resolution synchrotron radiation facilities, the experimental observation of very close CEBE values has become possible, as evidenced by the results of a recent investigation of the photoelectron spectra of propene and 2-methylpropene [51]. For the two reported conformers of lactonitrile, only a very small difference between their corresponding CEBEs was found. ESCA is, however, not capable of detecting small conformational changes [32], since they do not represent a substantial modification of the chemical environment.

4.3 Core-Electron Binding Energies of Si, P, S, Cl, and Ar

The results of the calculations of CEBEs of Si, P, S, Cl, and Ar are summarized in Tables 4-10 through 4-13. All the values reported correspond to ionization from $2p$ orbitals, which is the most common experimentally studied transition in the case of third-period elements. Most experimental data [40, 112] are for $2p_{3/2}$ energies — 3/2 is the value of the total angular momentum quantum number j, in the case of a $2p$ orbital j $(= l \pm s)$ is either

Table 4-10. Basis set convergence in the calculation of Si $2p$ energies (in eV). Experimental results are for $2p$ transitions.

molecule	cc-pVTZ	cc-pVQZ	cc-pV5Z	experiment
Si F_4	112.72	113.03	111.86	111.75
Si HCl_3	110.37	110.88	109.79	109.44
Si H_3Cl	108.95	109.70	108.65	108.11
Si H_3Br	108.91	109.51	108.45	108.08
Si H_2FCH_3	109.01	109.58	108.51	108.01
Si $_2H_6O$	108.83	109.41	108.36	107.81
Si $_2H_6S$	108.39	109.00	107.96	107.45
Si H_4	108.13	108.76	107.71	107.30
Si H_3CH_3	107.68	108.30	107.25	106.89

3/2 or 1/2 ($l = 1$, $s = 1/2$) — except for Si cases and some of the P, S, and Cl cases where weighted averages — these are referred to as $2p$ energies — of spin-orbit doublets have been reported [112].

Irregularities associated with the convergence of the cc-pVnZ basis sets are observed especially in the case of Si CEBEs but also in most P cases. It should also be noticed that although S and Cl CEBEs show the expected trend (TZ > QZ > 5Z), the convergence is considerably slower than it is in the case of calculations for second-period elements (Section 4.1). The existence of irregularities has been confirmed by Dunning [118], who has pointed out that some of the problems are due to deficiencies in the d-set, and has suggested augmenting the cc-pVnZ sets via addition of high-exponent d-functions. A

Table 4-11. Basis set convergence in the calculation of P $2p$ energies (in eV). Experimental results are for $2p_{3/2}$ transitions unless otherwise indicated.

molecule	cc-pVTZ	cc-pVQZ	cc-pV5Z	experiment
P F_5	145.39	145.35	144.25	144.65 $^{(2p)}$
P OF_3	144.20	144.18	143.10	143.25 $^{(2p)}$
				143.00
P SF_3	143.41	143.43	142.38	142.68 $^{(2p)}$
P F_3	142.78	142.87	141.93	142.05 $^{(2p)}$
				141.78
P F_3BH_3	143.46	143.53	142.53	141.79
P OCl_3	142.04	142.09	141.05	141.35 $^{(2p)}$
				141.02
P Cl_3	140.83	140.96	140.05	140.15 $^{(2p)}$
				139.75
P Cl_2CH_3	139.79	139.95	139.04	138.88 $^{(2p)}$
P H_3	138.21	138.44	137.57	137.33 $^{(2p)}$
				137.05
P H_2CH_3	137.83	137.98	137.10	136.55
$\mathbf{P}_4$	137.68	137.88	136.98	136.20

set of augmenting d-functions for sulphur (provided by Dunning [118]) was incorporated into the original cc-pVnZ basis sets (Section 3.2.1, Table 3-1) and was found to yield more accurate results. Therefore, all S CEBEs were

calculated with the augmented cc-pVnZ basis sets which differ from those described in Section 3.2.1 by the inclusion of one more d-function.

Table 4-12. Basis set convergence in the calculation of S $2p$ energies (in eV). Experimental results are for $2p_{3/2}$ transitions unless otherwise indicated.

molecule	cc-pVTZ	cc-pVQZ	cc-pV5Z	experiment
SF_6	180.69	180.52	179.90	181.00 [2p]
				180.29
SF_5Cl	179.93	179.77	179.15	179.27
SF_4	178.32	178.22	177.63	178.20 [2p]
SO_2F_2	178.52	178.39	177.78	177.67
NSF_3	177.79	177.67	177.07	176.97
SO_3	177.55	177.43	176.84	176.67
SOF_2	177.01	176.90	176.31	176.20
SO_2Cl_2	176.91	176.71	176.13	176.05
SO_2	175.83	175.63	175.06	174.82
$SOCl_2$	175.47	175.33	174.72	174.53
$(CH3)_2SO$	173.01	172.94	172.35	171.91
S_2Cl_2	172.63	172.48	171.88	171.57
OCS	172.35	172.22	171.63	170.69
H_2S	171.81	171.70	171.11	170.32
PSF_3	171.35	171.20	170.61	170.30 [2p]
CS_2	171.54	171.42	170.82	169.92
CH_3SH	171.10	170.98	170.39	169.40
$(CH_3)_2S$	170.55	170.44	169.85	169.06
$(SiH_3)_2S$	170.36	170.22	169.64	168.60

Table 4-13. Basis set convergence in the calculation of Ar and Cl $2p$ energies (in eV). Experimental results are for $2p_{3/2}$ transitions unless otherwise indicated.

molecule	cc-pVTZ	cc-pVQZ	cc-pV5Z	experiment
Ar	249.91	249.48	249.18	248.62
Cl FO_3	217.96	217.33	216.39	216.27
Cl F_3	214.19	213.87	213.35	213.02
Cl F	211.16	210.84	210.39	209.19
Cl $_2$	209.51	209.15	208.71	207.82
SO_2 **Cl** $_2$	208.84	208.50	208.07	207.49
SF_5 **Cl**	208.84	208.48	208.04	207.44
PO **Cl** $_3$	208.67	208.32	207.89	207.40 $^{(2p)}$
				207.32
H **Cl**	209.11	208.78	208.34	207.39
C **Cl** $_4$	208.38	208.07	207.62	207.02
B **Cl** $_3$	208.36	208.06	207.62	207.00
Si **Cl** $_4$	208.18	207.85	207.42	206.92
CH **Cl** $_3$	208.34	208.04	207.60	206.83
I **Cl**	208.22	207.85	207.40	206.68
CH_2 **Cl** $_2$	208.21	207.89	207.45	206.66
Ge **Cl** $_4$	207.97	207.62	207.19	206.65
P **Cl** $_3$	207.83	207.44	206.99	206.60 $^{(2p)}$
				206.42
SO **Cl** $_2$	207.88	207.52	207.08	206.55
CH_3 **Cl**	208.00	207.67	207.22	206.25
SiH_3 **Cl**	207.88	207.53	207.10	206.22
S_2 **Cl** $_2$	207.48	207.12	206.67	206.21
CrO_2 **Cl** $_2$	207.87	207.47	207.04	206.18
VO **Cl** $_3$	207.61	207.23	206.79	206.10
GeH_3 **Cl**	207.31	206.98	206.56	205.67

Average absolute deviations from experimental results are given in Tables 4-14 and 4-15. The AADs for Si and P CEBEs and the AADs from $2p$ energies (the vast majority of which are Si and P cases) clearly show the convergence irregularities in the basis sets. Calculations are in better agreement with experimental $2p$ energies than they are with $2p_{3/2}$ energies. This is related to the fact that the relativistic spin-orbit coupling effects which cause the splitting of the $2p$ transition into a doublet cannot be explicitly incorporated or treated in deMon calculations.

Table 4-14. Average Absolute Deviation (in eV) of calculated core-electron binding energies from experiment sorted by element. The number of test cases is given in parentheses.

basis set	**Si**	**P**	**S**	**Cl**
AAD from $2p$ energies				
cc-pVTZ	0.91 (9)	0.79 (8)		
cc-pVQZ	1.48 (9)	0.87 (8)		
cc-pV5Z	0.41 (9)	0.22 (8)		
AAD from $2p_{3/2}$ energies				
cc-pVTZ		1.24 (8)	1.12 (17)	1.50 (23)
cc-pVQZ		1.35 (8)	0.99 (17)	1.14 (23)
cc-pV5Z		0.40 (8)	0.45 (17)	0.68 (23)

Table 4-15. Average Absolute Deviation (in eV) of calculated core-electron binding energies from experiment for all test cases. The number of test cases is given in parentheses.

basis set	**AAD from $2p$ energies**	**AAD from $2p_{3/2}$ energies**
cc-pVTZ	0.84 (22)	1.32 (49)
cc-pVQZ	1.06 (22)	1.12 (49)
cc-pV5Z	0.38 (22)	0.55 (49)

In general, the results obtained with the cc-pV5Z basis sets are reasonably good, especially if the comparison is made with experimental $2p$ energies. In fact, the AAD (from $2p$ energies) for P cases (0.22 eV) is almost as good as the AAD obtained in calculations of CEBEs of second-period elements [18, 19, 20, 24], in which a larger number of cases were explored. However, the strongest (and, as reflected by the number of cases in Table 4-15, most frequently reported) transition is usually the ionization from the $2p_{3/2}$ level, with which calculated CEBEs do not agree so well, particularly for the Cl cases.

It is expected that the performance of the uGTS approach to the CEBEs of third-period elements will improve once the deficiencies in the basis set have been corrected and relativistic effects can be calculated or be available to be included as corrections to the calculated CEBEs.

Chapter 5

The ΔE-KS Approach: Test of Functionals

The unrestricted generalized transition state model, combined with density functional theory, has been shown to be an excellent approach to the calculation of core-electron binding energies of second-period elements (Chapter 4). Nevertheless, as discussed in Chapter 3, the uGTS model is an approximation to the exact core-ionization energies. This and the next chapter will explore the application of DFT to the determination of molecular CEBEs using the ΔE-KS method, in which no model error is introduced because calculations are performed for a fully ionized final state rather than for a transition state (as in the uGTS).

A set of seventeen cases, representing a reliable database of observed CEBEs, was selected to perform all the calculations reported in this chapter. The purpose of using this small database was to reduce experimental error. Each of the observed CEBEs has been measured (or recalibrated) at least

four times, and the value that is used for comparison with calculations was obtained by taking a weighted average of the corresponding experimental results, based on the reported (or estimated) uncertainties. Complete details about the CEBE database are given in the Appendix. All calculations were carried out at the experimental geometries [110].

Ten functional combinations — all available in deMon-KS [119] — were studied using the ΔE-KS procedure. The functional compositions are given in Table 5-1.

Table 5-1. Composition of exchange-correlation functionals.

functional	**exchange**	**correlation**
P86/P91	Perdew-Wang (1986)	Perdew-Wang (1991)
P86/P86	Perdew-Wang (1986)	Perdew (1986)
B88/P86	Becke (1988)	Perdew (1986)
P91/P86	Perdew-Wang (1991)	Perdew (1986)
B88/P91	Becke (1988)	Perdew-Wang (1991)
P91/P91	Perdew-Wang (1991)	Perdew-Wang (1991)
B88/LAP	Becke (1988)	Laplacian
P91/LAP	Perdew-Wang (1991)	Laplacian
P86/LAP	Perdew-Wang (1986)	Laplacian
LSD	LSD	Vosko-Wilk-Nusair

The functionals developed by Becke (B88 [88]), Perdew (correlation P86 [87]), and Perdew and Wang (exchange P86 [86], P91 [78]) are of the GGA type (discussed in Chapter 2, Section 2.2.2). The Laplacian functional [120] is a non-local generalization of a gradient-free correlation functional [121] designed to involve the kinetic energy density and hence the Laplacian of the electron density. The LSD functional tested employs the Vosko-Wilk-Nusair parametrization [80] for the correlation energy.

5.1 Model Error and Functional Error

In the uGTS/DFT method, the deviation of the calculated CEBEs from the observed values can be represented as follows

$$deviation = EE + ME + RCE + BSE + FE \tag{5.1}$$

where the terms on the right-hand side are the experimental error (EE), the model error (ME), the relativistic correction error (RCE), the basis set error (BSE), and the functional error (FE), respectively. ME is obtained as the difference between the uGTS result and the ΔE-KS result. RCE is assumed to be negligible, and so are EE and BSE. The justification for neglecting the experimental and basis set errors is that the calculations were limited to the aforementioned database of reliable observed CEBEs, and were carried out with the cc-pV5Z basis sets (which have been shown to perform almost as efficiently as a complete basis set [20, 24]). FE is calculated from equation (5.1) after the deviation and the model error have been determined from the

results of the DFT calculations.

Table 5-2. Error analysis (in eV) for uGTS calculations with the B88/P86 functional.

molecule	deviation	model error	functional error
CO	+0.17	0.49	−0.32
CO_2	−0.35	0.53	−0.88
CH_4	+0.12	0.65	−0.53
CF_4	−0.59	0.62	−1.21
CCl_4	+0.01	0.74	−0.73
C$_2H_6$	+0.12	0.57	−0.45
N$_2$	+0.09	0.49	−0.40
N**N**O	−0.08	0.58	−0.66
NNO	−0.04	0.53	−0.57
CH_3C**N**	0.00	0.67	−0.67
C**O**	+0.17	0.66	−0.49
C**O**$_2$	+0.10	0.66	−0.56
H_2**O**	+0.14	0.67	−0.53
HC**O**OH	−0.08	0.70	−0.78
HCO**O**H	+0.19	0.70	−0.51
CH_3**O**H	+0.08	0.80	−0.72
C**F**$_4$	−0.42	0.77	−1.19

Table 5-3. Error analysis (in eV) for uGTS calculations with the P86/P86 functional.

molecule	deviation	model error	functional error
CO	0.85	0.57	+0.28
CO_2	0.35	0.51	−0.16
CH_4	0.87	0.66	+0.21
CF_4	0.11	0.58	−0.47
CCl_4	0.69	0.75	−0.06
C$_2H_6$	0.85	0.60	+0.25
N$_2$	0.93	0.65	+0.28
N**N**O	0.79	0.63	+0.16
NNO	0.79	0.64	+0.15
CH_3C**N**	0.88	0.67	+0.21
C**O**	1.10	0.66	+0.44
C**O**$_2$	0.87	0.51	+0.36
H_2**O**	1.10	0.76	+0.34
HC**O**OH	0.88	0.71	+0.17
HCO**O**H	1.12	0.71	+0.41
CH_3**O**H	1.01	0.77	+0.24
C**F**$_4$	0.63	0.74	−0.11

In the original study conducted by Chong [18], three of the functionals given in Table 5-1 were tested: B88/P86, P86/P86, and LSD. An error anal-

ysis based on equation (5.1) was carried out for each of them and the results are shown in Tables 5-2, 5-3, and 5-4.

Table 5-4. Error analysis (in eV) for uGTS calculations with the LSD functional.

molecule	deviation	model error	functional error
C O	−3.05	0.44	−3.49
C O_2	−3.65	0.48	−4.13
C H_4	−3.45	0.53	−3.98
C F_4	−3.93	0.46	−4.39
C Cl_4	−3.31	0.43	−3.74
C$_2H_6$	−3.40	0.51	−3.91
N$_2$	−3.87	0.49	−4.36
N **N** O	−4.03	0.49	−4.52
N NO	−4.02	0.49	−4.51
CH_3C **N**	−4.02	0.54	−4.56
C **O**	−4.44	0.55	−4.99
C **O**$_2$	−4.55	0.55	−5.10
H_2 **O**	−4.72	0.61	−5.33
HC **O** OH	−4.73	0.55	−5.28
HCO **O** H	−4.52	0.57	−5.09
CH_3 **O** H	−4.67	0.62	−5.29
C **F**$_4$	−5.68	0.60	−6.28

The reason the B88/P86 functional performs so well in uGTS calculations of CEBEs is clear from examination of Table 5-2. The model error is always a positive quantity whereas the functional error is always negative. This results in a fortuitous partial cancellation of errors which helps to produce calculated energies in impressive agreement with observed values. For the 17 cases in the database, the AAD from experiment is only 0.17 eV.

The functional error of the P86/P86 combination is smaller than that of the B88/P86 functional but it is a positive quantity for most of the cases investigated (Table 5-3). Therefore, the functional error adds to the model error and causes the performance of P86/P86 to be considerably inferior — the AAD from experiment is 0.82 eV — to that of B88/P86.

The LSD had been found to be incapable of yielding CEBEs with acceptable accuracy [18]. Table 5-4 shows that this is due to a large error associated with the functional itself, which leads to a notable underestimation of the core-ionization energies.

5.2 Functional Performance in ΔE-KS Calculations

The results of the study of the ten functional combinations using the ΔE-KS procedure are presented in this Section. Table 5-5 shows their performance analyzed on the basis of the deviations of the calculated CEBEs from the corresponding experimental values.

The combination of the Perdew-Wang functionals (P86/P91) yielded the best results with an AAD from experiment of 0.15 eV, and surpassed the performance of B88/P86 in the uGTS approach whose AAD was 0.17 eV

Table 5-5. Average Absolute Deviation (in eV) and Maximum Deviation (in eV) of the core-electron binding energies (calculated with the functionals in Table 5-1) from experiment. All results include data from the 17 cases in the database, except for the P91/P86 and P91/LAP results which include 15 cases (calculations for CCl_4 and C_2H_6 failed to converge).

functional	AAD	MD
P86/P91	0.15	−0.66
P86/P86	0.26	−0.47
B88/P86	0.65	−1.21
P91/P86	0.66	−1.11
B88/P91	0.81	−1.44
P91/P91	0.87	−1.40
B88/LAP	0.88	+1.14
P91/LAP	0.91	+1.16
P86/LAP	1.67	+2.05
LSD	4.64	−6.27

(Section 5.1). This is a particularly important result because the model error had already been eliminated (by employing the ΔE-KS method) and a functional has been found that leads to a sufficiently small error to provide highly accurate CEBEs. The core-ionization energies for each of the database cases (obtained with the P86/P91 functional) are shown in Table 5-6. Except for the carbon cases in CO_2 and CF_4, and the fluorine case, all the CEBEs

deviate from the observed values by 0.20 eV at most. In fact, if these three "problem" cases were ignored, the AAD would drop to 0.08 eV.

Table 5-6. Core-electron binding energies (in eV) calculated with the P86/P91 functional. Calculated CEBEs include relativistic corrections from equation (4.1).

molecule	CEBE	experiment
C O	296.25	296.21
C O_2	297.28	297.69
C H_4	290.87	290.84
C F_4	301.23	301.89
C Cl_4	296.35	296.36
C $_2H_6$	290.75	290.72
N $_2$	410.01	409.98
N **N** O	412.52	412.59
N NO	408.59	408.71
CH_3C **N**	405.53	405.64
C **O**	542.73	542.55
C **O** $_2$	541.36	541.28
H_2 **O**	539.98	539.90
HC **O** OH	538.86	538.97
HCO **O** H	540.83	540.63
CH_3 **O** H	539.09	539.11
C **F** $_4$	695.14	695.56

The performance of the Perdew-Wang-Perdew (P86/P86) combination is also good and represents a remarkable improvement upon the uGTS results obtained with this functional (AAD of 0.26 eV for ΔE-KS compared with AAD of 0.82 eV for uGTS). On the other hand, the performance of the B88/P86 degraded considerably (from an AAD of 0.17 eV for uGTS to an AAD of 0.65 eV for ΔE-KS). Both results are consistent with the observations made in the previous section.

Chapter 6

The ΔE-KS Approach: Test of Basis Sets

The results presented in Chapter 5 have shown that the P86/P91 functional combination is the best option for DFT calculations of CEBEs within the ΔE-KS approach. The tests were carried out with a highly efficient though large (computationally demanding) basis set. It was pointed out in Chapter 3 that the use of smaller basis sets is essential to extend calculations to increasingly large systems as the ultimate goal is to be able to treat systems which can serve as realistic models for extended structures such as polymers and surfaces, on which most current experimental investigations are being focused.

A number of possible alternatives to the cc-pV5Z set (which was the only basis used in the initial tests) were considered in Section 3.2.1, and their performances will be presented and discussed in this chapter.

All calculations reported in this chapter were performed with the P86/P91

functional at the experimental geometries of the neutral parent molecules [110]. The database introduced in Chapter 5 was employed as well as some additional fluorine cases (there is only one case in the database) and some boron cases (not represented in the database). Only for HF was it possible to obtain a weighted average (details are given in the Appendix).

6.1 Scaled Basis Sets

A convergence study was carried out for the cc-pVnZ basis sets and the results are shown in Table 6-1. The estimated complete basis set limits were calculated using equation (4.2). It is observed that the cc-pV5Z set is indeed highly efficient as evidenced by the fact that except for the O case in CO (with a deviation of only 0.01 eV) all the CEBEs are equal to the corresponding CBS limits.

Table 6-2 summarizes the results of calculations carried out with the scaled basis sets constructed by means of the three different scaling procedures described by equations (3.25) through (3.29), and compares their performances with the CBS limits (from Table 6-1) and with the experimental energies. A more general analysis, based on deviations from both experiment and CBS, of all six basis sets studied is given in Table 6-3.

The average absolute deviations indicate that exponent scaling is not an effective means of describing the core-hole state in the ΔE-KS method, in contrast to the results obtained in uGTS calculations (Section 4.1). In fact, only one of the scaled basis sets (III-pVTZ) has consistently improved upon the AADs of the original cc-pVTZ sets, but the extent of improvement is

Table 6-1. Basis set convergence in ΔE-KS/P86-P91 calculations of core-electron binding energies (in eV). Calculated CEBEs include relativistic corrections from equation (4.1).

molecule	cc-pVTZ	cc-pVQZ	cc-pV5Z	CBS	experiment
C O	296.55	296.28	296.25	296.25	296.21
C O_2	297.54	297.31	297.28	297.28	297.69
C H_4	291.19	290.90	290.87	290.87	290.84
C F_4	301.46	301.24	301.23	301.23	301.89
C Cl_4	296.77	296.39	296.35	296.35	296.36
C $_2H_6$	291.08	291.78	290.75	290.75	290.72
N $_2$	410.34	410.04	410.01	410.01	409.98
N **N** O	412.83	412.54	412.52	412.52	412.59
N NO	408.90	408.61	408.59	408.59	408.71
CH_3C **N**	405.88	405.56	405.53	405.53	405.64
C **O**	543.17	542.78	542.73	542.72	542.55
C **O** $_2$	541.77	541.40	541.36	541.36	541.28
H_2 **O**	540.29	539.98	539.98	539.98	539.90
HC **O** OH	539.24	538.88	538.86	538.86	538.97
HCO **O** H	541.23	540.86	540.83	540.83	540.63
CH_3 **O** H	539.47	539.11	539.09	539.09	539.11
C **F** $_4$	695.60	695.18	695.14	695.14	695.56
H **F**	694.62	694.27	694.26	694.26	694.23
Cl **F**	694.80	694.36	694.32	694.32	694.36
B **F** $_3$	695.10	694.65	694.60	694.59	694.80
F $_2$	696.98	696.56	696.52	696.52	696.69
B F_3	202.36	202.13	202.10	202.10	202.80
B $_2H_6$	196.67	196.42	196.40	196.40	196.50
B H_3CO	195.40	195.16	195.14	195.14	195.10
B H_3NH_3	194.25	193.97	193.94	193.94	193.73

Table 6-2. ΔE-KS/P86-P91 calculations of core-electron binding energies (in eV) with scaled basis sets. Calculated CEBEs include relativistic corrections from equation (4.1).

molecule	I-pVTZ	II-pVTZ	III-pVTZ	CBS	experiment
C O	296.68	296.67	296.65	296.25	296.21
C O_2	297.55	297.55	297.54	297.28	297.69
C H_4	291.03	291.02	291.01	290.87	290.84
C F_4	301.35	301.35	301.35	301.23	301.89
C Cl_4	296.45	296.44	296.43	296.35	296.36
C $_2H_6$	290.87	290.86	290.86	290.75	290.72
N $_2$	410.42	410.40	410.33	410.01	409.98
N **N** O	412.73	412.72	412.71	412.52	412.59
N NO	408.88	408.84	408.76	408.59	408.71
CH_3C **N**	405.79	405.76	405.71	405.53	405.64
C **O**	543.20	543.17	543.12	542.72	542.55
C **O** $_2$	541.79	541.77	541.70	541.36	541.28
H_2 **O**	540.39	540.35	540.28	539.98	539.90
HC **O** OH	539.27	539.23	539.16	538.86	538.97
HCO **O** H	541.22	541.19	541.12	540.83	540.63
CH_3 **O** H	539.50	539.47	539.39	539.09	539.11
C **F** $_4$	695.68	695.64	695.54	695.14	695.56
H **F**	694.78	694.73	694.63	694.26	694.23
Cl **F**	694.96	694.92	694.82	694.32	694.36
B **F** $_3$	695.15	695.11	695.01	694.59	694.80
F $_2$	697.19	697.14	697.04	696.52	696.69
B F_3	202.44	202.44	202.42	202.10	202.80
B $_2H_6$	196.67	196.67	196.67	196.40	196.50
B H_3CO	195.39	195.39	195.39	195.14	195.10
B H_3NH_3	194.25	194.21	194.21	193.94	193.73

Table 6-3. Average Absolute Deviation (in eV) of calculated core-electron binding energies from experiment and from CBS. The number of test cases is given in parentheses.

basis set	**AAD** from experiment	**AAD** from CBS
	database cases (17)	
cc-pVTZ	0.30	0.33
cc-pVQZ	0.16	0.03
cc-pV5Z	0.15	0.00
I-pVTZ	0.33	0.32
II-pVTZ	0.30	0.30
III-pVTZ	0.26	0.25
CBS	0.15	
	all test cases (25)	
cc-pVTZ	0.35	0.34
cc-pVQZ	0.16	0.03
cc-pV5Z	0.16	0.00
I-pVTZ	0.35	0.36
II-pVTZ	0.33	0.34
III-pVTZ	0.29	0.29
CBS	0.16	

still not significant (especially if compared with uGTS results). Examination of the individual molecules reveals that, in general, B, O, and F CEBEs are difficult cases for the scaled basis sets. The I-pVTZ and II-pVTZ sets do

not perform satisfactorily at all, and the performance of the III-pVTZ set is acceptable only for some of the cases. Results are reasonably good for "sp^3" C cases and for most N cases (the N_2 CEBE is the only definitely poor result among the four cases studied), but C atoms involved in multiple bonds appear to be problematic (the CO molecule in particular).

The difference between the I/II sets and the III sets lies in that I and II separate the effects of $1s$- and $2s$-electrons on the screening factor for the $2p$ functions whereas no such partition is included in III. The fact that the performance of the III-pVTZ basis set is better than that of the I/II-pVTZ sets suggests that, as far as shielding effects on $2p$-electrons are concerned, treating $1s$- and $2s$-electrons as a whole may be a more efficient way of describing the core-hole state in the ΔE-KS method.

6.2 Core-Valence Correlated Basis Sets

It was mentioned in Chapter 3 that the core-valence correlated basis functions labeled as cc-pCVTZ [109] were another possible alternative to the use of the large cc-pV5Z set. Therefore, they were also tested in ΔE-KS calculations of core-electron binding energies. A summary of the results obtained is given in Table 6-4 and a comparison with cc-pVTZ and cc-pV5Z results is presented in Table 6-5.

A significant improvement upon the cc-pVTZ results was achieved when the calculations were carried out using cc-pCVTZ basis functions (the AAD decreased more than half for all test cases in Table 6-4). It should be noted that although the cc-pCVTZ basis set is an augmented version of the original

Table 6-4. ΔE-KS/P86-P91 calculations of core-electron binding energies (in eV) with cc-pCVTZ basis sets. Calculated CEBEs include relativistic corrections from equation (4.1).

molecule	cc-pCVTZ	experiment
CO	296.27	296.21
CO_2	297.28	297.69
CH_4	290.93	290.84
CF_4	301.17	301.89
CCl_4	296.45	296.36
C$_2H_6$	290.80	290.72
N$_2$	410.05	409.98
N**N**O	412.55	412.59
NNO	408.62	408.71
CH_3C**N**	405.60	405.64
C**O**	542.84	542.55
C**O**$_2$	541.44	541.28
H_2**O**	539.95	539.90
HC**O**OH	538.90	538.97
HCO**O**H	540.88	540.63
CH_3**O**H	539.12	539.11
C**F**$_4$	695.23	695.56
H**F**	694.26	694.23
Cl**F**	694.43	694.36
B**F**$_3$	694.74	694.80
F$_2$	696.61	696.69
BF_3	202.12	202.80
B$_2H_6$	196.43	196.50
BH_3CO	195.17	195.10
BH_3NH_3	193.98	193.73

Table 6-5. Average Absolute Deviation (in eV) of calculated core-electron binding energies from experiment. The number of test cases is given in parentheses.

basis set	**AAD** from experiment
database cases (17)	
cc-pVTZ	0.30
cc-pCVTZ	0.17
cc-pV5Z	0.15
all test cases (25)	
cc-pVTZ	0.35
cc-pCVTZ	0.17
cc-pV5Z	0.16

cc-pVTZ set (Section 3.2.1) the results are still remarkable in that they almost reproduce the AADs of the cc-pV5Z set which is considerably more demanding in computational terms. Moreover, for the database cases, the AAD of the cc-pCVTZ results is equal to the AAD obtained in the uGTS/B88-P86 calculations with the cc-pV5Z basis sets (Chapter 5).

The results of additional calculations performed with cc-pVTZ and cc-pCVTZ basis set are reported in Table 6-6. Seven molecules — all of which are larger than the species that comprise the test cases of the previous section — were studied, and the results obtained were highly accurate with an AAD from experiment of 0.07 eV and of 0.19 eV for cc-pCVTZ and cc-pVTZ, respectively.

If all 32 cases studied with the cc-pCVTZ basis set are considered, then the AAD from experiment is 0.15 eV, exactly the same as the AAD obtained for the 17 database cases with the cc-pV5Z basis set.

Table 6-6. Calculations of core-electron binding energies (in eV) of larger molecules. Calculated CEBEs include relativistic corrections from equation (4.1). The experimental data for the aromatic compounds are a weighted average of the observed CEBEs (details are given in the Appendix).

molecules	cc-pVTZ	cc-pCVTZ	experiment
$\mathbf{B}_5H_9$ – *apex*	194.27	194.11	194.20
$\mathbf{B}_5H_9$ – *base*	196.30	196.11	196.10
$\mathbf{C}_6H_6$	290.58	290.33	290.39
$\mathbf{C}_6H_5NH_2$	291.51	291.25	291.37
$\mathbf{C}_6H_5F$	292.91	292.66	292.75
$C_6H_5\,\mathbf{N}\,H_2$	405.72	405.42	405.40
$C_6H_5\,\mathbf{F}$	693.15	692.79	692.92

Further insight into the performance of basis sets can be gained by means of completeness profiles [122, 123]. The completeness profile of a basis set is defined as the sum of the squares of the overlap of a test normalized Gaussian function with an orthonormalized basis [122]. If the test Gaussian is represented as $G(\alpha)$ — where α is a variable exponent — and $\{\psi_k\}$ is a

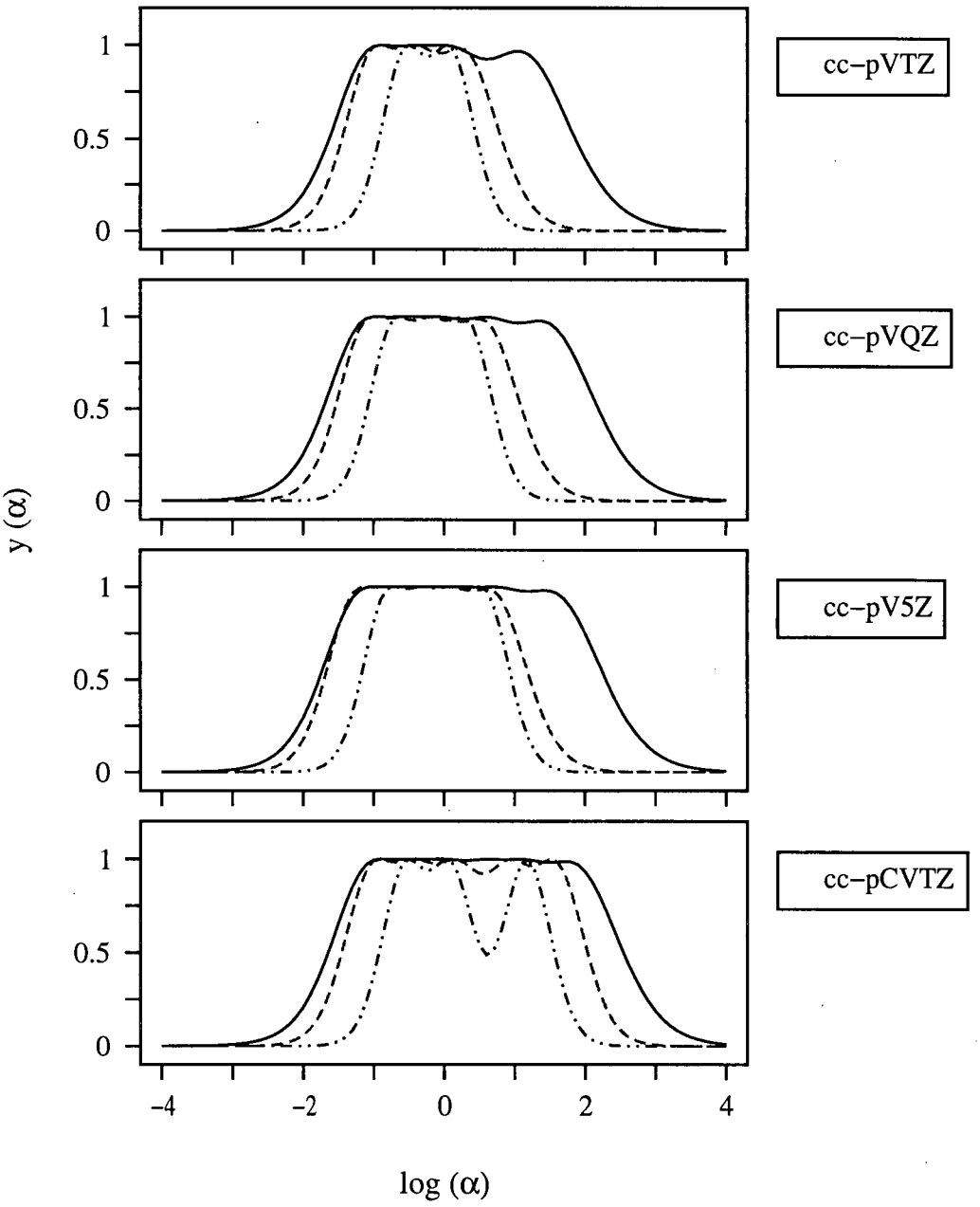

Figure 6-1. Completeness profiles of cc-pVnZ and cc-pCVTZ basis sets; s-functions: solid, p-functions: dash, d-functions: dot-dash.

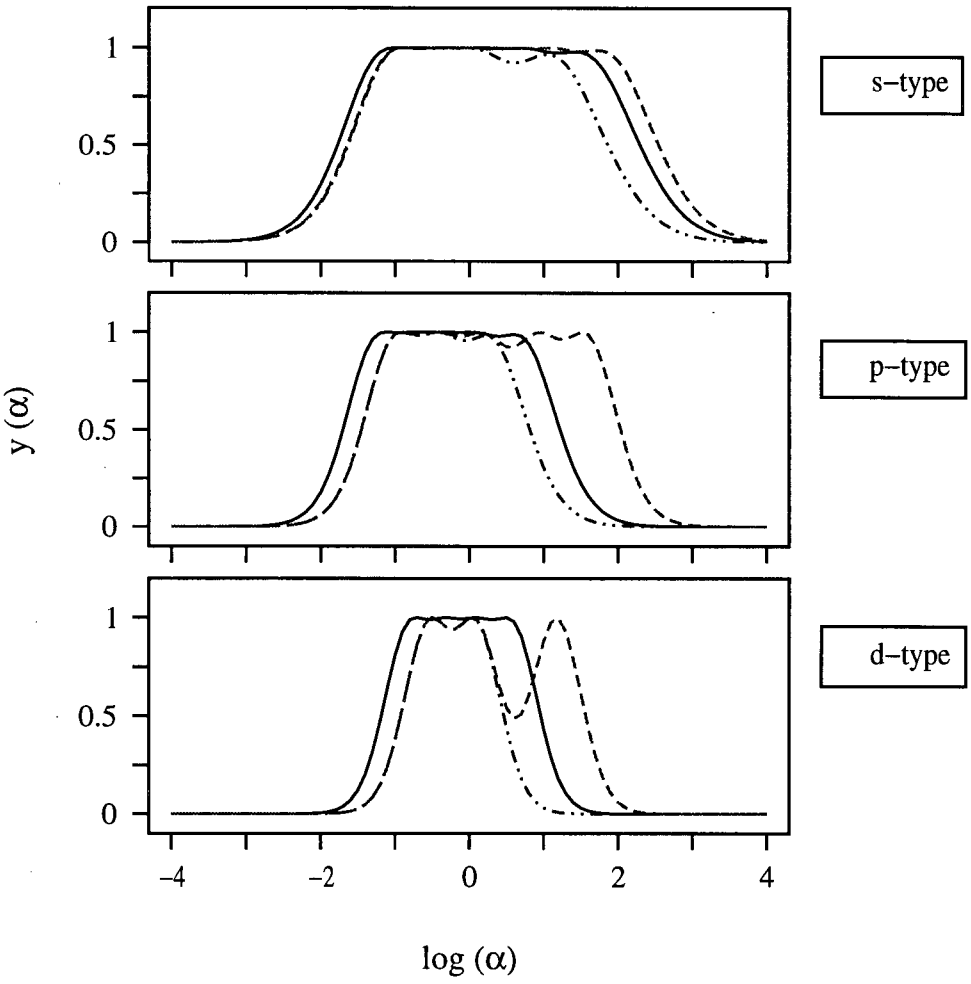

Figure 6-2. Comparison of completeness profiles for the *s*-, *p*-, and *d*-type functions of cc-pVTZ (dot-dash), cc-pV5Z (solid), and cc-pCVTZ (dash) basis sets.

generic set of orthonormalized basis functions, then the completeness profile is a plot of $Y(\alpha)$ as a function of $x = log(\alpha)$, with $Y(\alpha)$ given by

$$Y(\alpha) = \sum < G(\alpha)|\psi_k >< \psi_k|G(\alpha) > \tag{6.1}$$

Completeness profiles for the cc-pVnZ and cc-pCVTZ basis sets are shown in Figure 6-1. A comparison of the profiles for the s-, p-, and d-type functions is presented in Figure 6-2. The profiles have been calculated only for the carbon atom, but they are expected to be qualitatively similar for the other second-period elements [123].

The closer the value of $Y(\alpha)$ is to 1.0, the more completely is the space spanned by the basis. The tight region is represented by high x values whereas low x values are associated with the diffuse (bonding) region. It is observed that at high $x = log(\alpha)$ the cc-pCVTZ set shows appreciably higher completeness than does the cc-pVTZ set — this tends to lead to better energies [123] — and also provides more adequate coverage than the cc-pV5Z set. Thus, the behaviour of the basis sets, as displayed by the completeness profiles, is in accord with the AAD-based results and supports the fact that the cc-pCVTZ basis set is an appropriate choice for density functional calculations of CEBEs.

A limited number of tests were carried out with a core-valence correlated basis set of double-zeta quality. This cc-pCVDZ set [109] is similar in composition to the cc-pVTZ set — [4s3p1d] compared to [4s3p2d] — so it was thought to be perhaps capable of providing good CEBEs at reduced computational effort. However, the results for seven of the database cases were rather unsatisfactory, the deviations from experiment ranging from 0.68 eV to 1.65 eV.

Chapter 7

Conclusion

This thesis has extended the computational approach to the determination of molecular core-electron binding energies introduced by Chong, the unrestricted generalized transition state model combined with density functional theory, by applying it to the calculation of CEBEs of boron-containing molecules, of isomers of C_3H_5NO, and of the third-period elements silicon, phosphorus, sulphur, chlorine, and argon.

The results obtained for boron were in very good agreement with experimental observations, for calculations performed both with large basis sets (cc-pV5Z) and with smaller but efficient basis sets (scaled-pVTZ). The scaled-pVTZ calculations for boron 1s energies gave an average absolute deviation of 0.07 eV from the estimated complete basis set limit, confirming that exponent-scaling is a highly effective method for improving basis-set performance in the treatment of partial core-hole states.

The extension of the original scaling methodology, in which the use of scaled basis functions is restricted to the atom with the core hole, to a generalized-scaling method, requiring scaled basis sets for every atom, was found not to be advantageous. The effort involved in calculating scaling factors for all the atomic centers in a molecule is too intensive to justify the limited improvement attained.

The calculated core-ionization energies of the isomers of C_3H_5NO clearly revealed the distinctive nature of the core-electron spectrum of the individual species. This and previous results, in conjunction with the fact that synchrotron-radiation instrumentation has already achieved sufficiently high resolution to distinguish atoms in remarkably similar environments, continue to support the traditional application of combined experimental and theoretical approaches to core-electron spectroscopy for the purpose of chemical and structural analysis.

The results for CEBEs of the third-period elements were in most cases of acceptable accuracy for calculations performed with the cc-pV5Z basis sets, but the deviations from observed values were found to be, in general, more than twice as large as those obtained for the second-period elements. A number of factors were recognized as (partially) responsible for the deficiencies detected, notably irregularities associated with the basis sets employed, and also absence of a (at least approximate) relativistic treatment.

This thesis has also tested a total-energy difference approach, within Kohn-Sham density functional theory, to calculating core-ionization energies. It was found that the remarkable success of uGTS/DFT calculations employing Becke's 1988 exchange functional and Perdew's 1986 correlation

functional was due to a fortuitous cancellation of the errors associated with the model (uGTS) and the functional. For the ΔE-KS method, the combination of Perdew and Wang's 1986 exchange and 1991 correlation functionals proved the most accurate among the ten functional options tested.

Exponent scaling was found not to be an adequate procedure for improving the performance of basis sets in ΔE-KS calculations. Therefore, a core-valence correlated basis set (cc-pCVTZ) was tested and found to be highly efficient with an average absolute deviation from experiment of 0.15 eV. The cc-pCVTZ basis set is smaller than the cc-pV5Z basis set, thus enabling calculations on relatively larger molecules.

The investigations reported in this thesis involving the use of the ΔE-KS approach should be considered to be in their preliminary stages. The most significant aspect is that the elimination of the model error and the small error of the Perdew-Wang functionals have made it possible to (slightly) surpass the already remarkable accuracy achieved with the uGTS method. Many applications remain to be explored, such as the extension to model systems for polymers and surfaces, the testing of the recently proposed second-order gradient functionals, and the analysis of the vibrational fine structure of core-electron spectra.

References

1. R. G. Parr, W. Yang, *Density-Functional Theory of Atoms and Molecules*, Oxford University Press. New York (1989)

2. P. Hohenberg, W. Kohn, Phys. Rev. **136**, B864 (1964)

3. W. Kohn, L. J. Sham, Phys. Rev. **140**, A1133 (1965)

4. P. Fulde, *Electron Correlations in Molecules and Solids*, 2nd Edition, Springer-Verlag, Berlin (1995)

5. W. Kohn, in *Recent Advances in Density Functional Methods, Part I*, edited by D. P. Chong, World Scientific, Singapore (1995)

6. J. K. Labanowski, J. W. Andzelm, editors, *Density Functional Methods in Chemistry*, Springer-Verlag, New York (1991)

7. T. Ziegler, Chem. Rev. **91**, 651 (1991)

8. D. P. Chong, editor, *Recent Advances in Density Functional Methods, Part I*, World Scientific, Singapore (1995)

9. R. G. Parr, W. Yang, Annu. Rev. Phys. Chem. **46**, 701 (1995)

10. B. B. Laird, R. B. Ross, T. Ziegler, editors, *Chemical Applications of Density-Functional Theory*, ACS, Washington, DC (1996)

11. W. Kohn, A. D. Becke, R. G. Parr, J. Phys. Chem. **100**, 12974 (1996)

12. D. P. Chong, editor, *Recent Advances in Density Functional Methods, Part II*, World Scientific, Singapore (1997)

13. E. J. Baerends, O. V. Gritsenko, J. Phys. Chem. **101**, 5383 (1997)

14. D. Joubert, editor, *Density Functionals: Theory and Applications*, Springer-Verlag, Berlin (1998)

15. Á. Nagy, Phys. Rep. **298**, 1 (1998)

16. M. Head-Gordon, J. Phys. Chem. **100**, 13213 (1996)

17. H. F. Schaefer, Theochem **398-399**, 199 (1997)

18. D. P. Chong, Chem. Phys. Letters **232**, 486 (1995)

19. D. P. Chong, J. Chem. Phys. **103**, 1842 (1995)

20. D. P. Chong, C-H. Hu, P. Duffy, Chem. Phys. Letters **249**, 491 (1996)

21. D. P. Chong, Can. J. Chem. **74**, 1005 (1996)

22. C-H. Hu, D. P. Chong, Chem. Phys. Letters **262**, 733 (1996)

23. K. Endo, Y. Kaneda, H. Okada, D. P. Chong, P. Duffy, J. Phys. Chem. **100**, 19455 (1996)

24. M. Pulfer, C-H. Hu, D. P. Chong, Chem. Phys. **216**, 91 (1997)

25. C-H. Hu, D. P. Chong, Chem. Phys. **216**, 99 (1997)

26. C. Bureau, D. P. Chong, Chem. Phys. Letters **264**, 186 (1997)

27. S. Kranias, C. Bureau, D. P. Chong, V. Brenner, I. George, P. Viel, G. Lecayon, J. Phys. Chem. B **101**, 10254 (1997)

28. C. Bureau, D. P. Chong, G. Lecayon, J. Delhalle, J. Electron Spectrosc. Rel. Phenom. **83**, 227 (1997)

29. D. P. Chong, C-H. Hu, J. Chem. Phys. **108**, 8950 (1998)

30. S. Hüfner, *Photoelectron Spectroscopy: Principles and Applications*, 2nd Edition, Springer-Verlag, Berlin (1996)

31. T. A. Carlson, *Photoelectron and Auger Spectroscopy*, Plenum Press, New York (1975)

32. A. D. Baker, *Photoelectron Spectroscopy: Chemical and Analytical Aspects*, Pergamon of Canada, Toronto (1972)

33. D. A. Shirley, Adv. Chem. Phys. **23**, 85 (1973)

34. D. Menzel, Surf. Sci. **299-300**, 170 (1994)

35. I. Jirka, J. Phys. Chem. B **101**, 8133 (1997)

36. T. Kugler, M. Logdlund, W. R. Salanek, Acc. Chem. Res. **32**, 225 (1999)

37. W. L. Jolly, Acc. Chem. Res. **16**, 370 (1983)

38. D. B. Beach, W. L. Jolly, Inorg. Chem. **23**, 4774 (1984)

39. D. B. Beach, W. L. Jolly, R. Mews, A. Waterfeld, Inorg. Chem. **23**, 4080 (1984)

40. D. B. Beach, W. L. Jolly, Inorg. Chem. **24**, 567 (1985)

41. A. Greenberg, T. D. Thomas, C. R. Bevilacqua, M. Coville, D. Ji, J-C. Tsai, G. Wu, J. Org. Chem. **57**, 7093 (1992)

42. L. J. Sæthre, T. D. Thomas, S. Svensson, J. Chem. Soc. Perkin Trans. II **4**, 749 (1997)

43. P. G. Gassman, P. A. Deck, Organometallics **13**, 2890 (1994)

44. H. Ågren, Int. J. Quant. Chem. **29**, 455 (1991)

45. U. Gelius, S. Svensson, H. Siegbahn, E. Basilier, Å. Faxälv, K. Siegbahn, Chem. Phys. Letters **28**, 1 (1974)

46. L. Asplund, U. Gelius, S. Hedman, K. Helenelund, K. Siegbahn, P. E. M. Siegbahn, J. Phys. B **18**, 1569 (1985)

47. G. L. Gutsev, A. I. Boldyrev, J. Electron Spectrosc. Rel. Phenom. **50**, 103 (1990)

48. A. Naves de Brito, N. Correia, S. Svensson, H. Ågren, J. Chem. Phys. **95**, 2965 (1991)

49. A. Naves de Brito, S. Svensson, H. Ågren, J. Delhalle, J. Electron Spectrosc. Rel. Phenom. **63**, 239 (1993)

50. S. J. Osborne, S. Sundin, A. Ausmees, S. Svensson, L. J. Sæthre, O. Sværen, S. L. Sorensen, J. Végh, J. Karvonen, S. Aksela, A. Kikas, J. Chem. Phys. **106**, 1661 (1997)

51. L. J. Sæthre, O. Sværen, S. Svensson, S. Osborne, T. D. Thomas, J. Jauhiainen, S. Aksela, Phys. Rev. A **55**, 2748 (1997)

52. S. Sundin, L. J. Sæthre, S. L. Sorensen, A. Ausmees, S. Svensson, J. Chem. Phys. **110**, 5806 (1999)

53. P. S. Bagus, Phys. Rev. **139**, A619 (1965)

54. M. E. Schwartz, in *Applications of Electronic Structure Theory*, edited by H. F. Schaefer, Plenum Press, New York (1977)

55. P. S. Bagus, D. Coolbaugh, S. P. Kowalczick, G. Pacchioni, F. Parmigiani, J. Electron Spectrosc. Rel. Phenom. **51**, 69 (1990)

56. U. Birkenheuer, F. Cora, C. Pisani, E. Scorza, G. Perego, Surf. Sci. **373**, 393 (1997)

57. A. E. de Oliveira, P. H. Guadagnini, R. Custódio, R. E. Bruns, J. Phys. Chem. A **102**, 4615 (1998)

58. W. Meyer, J. Chem. Phys. **58**, 1017 (1973)

59. D. A. Shirley, Chem. Phys. Letters **16**, 220 (1972)

60. H. Basch, J. Electron Spectrosc. Rel. Phenom. **5**, 463 (1974)

61. Y. Chen, G. Zhuang, P. N. Ross, M. A. Van Hove, C. S. Fadley, J. Chem. Phys. **109**, 6527 (1998)

62. J. C. Slater, Adv. Quantum Chem. **6**, 1 (1972)

63. D. P. Chong, T. Minato, P. K. Mukherjee, Int. J. Quant. Chem. **23**, 1903 (1983)

64. D. P. Chong, P. K. Mukherjee, Chem. Phys. Letters **94**, 383 (1983)

65. P. K. Mukherjee, D. P. Chong, Chem. Phys. Letters **120**, 163 (1985)

66. D. Hening, M. V. Ganduglia-Pirovano, M. Scheffler, Phys. Rev. B **53**, 10344 (1996)

67. L. Pedocchi, M. R. Ji, S. Lizzit, G. Comelli, G. Rovida, J. Electron Spectrosc. Rel. Phenom. **76**, 383 (1995)

68. C. Bureau, Chem. Phys. Letters **269**, 378 (1997)

69. A. R. Williams, R. A. deGroot, C. B. Sommers, J. Chem. Phys. **63**, 628 (1975)

70. P. W. Atkins, R. S. Friedman, *Molecular Quantum Mechanics*, 3rd Edition, Oxford University Press, Oxford (1997)

71. J. Sadlej, *Semi-empirical Methods of Quantum Chemistry*, Ellis Horwood Limited, Chichester (1985)

72. J. A. Pople, D. L. Beveridge, *Approximate Molecular Orbital Theory*, McGraw-Hill, USA (1970)

73. A. Szabo, N. S. Ostlund, *Modern Quantum Chemistry*, Dover, New York (1996)

74. R. M. Dreizler, E. K. U. Gross, *Density Functional Theory*, Springer-Verlag, Berlin (1990)

75. E. Steiner, *The Chemistry Maths Book*, Oxford University Press, New York (1996)

76. M. Born, J. R. Oppenheimer, Ann. Physik **84**, 457 (1927)

77. J. Simons, J. Phys. Chem. **95**, 1017 (1991)

78. J. P. Perdew, S. Kurth, in *Density Functionals: Theory and Applications*, edited by D. Joubert, Springer-Verlag, Berlin (1998)

79. J. P. Perdew, A. Zunger, Phys. Rev. B **23**, 5048 (1981)

80. S. H. Vosko, L. Wilk, M. Nusair, Can. J. Phys. **58**, 1200 (1980)

81. A. G. Koures, F. E. Harris, Int. J. Quantum Chem. **59**, 3 (1996)

82. D. M. Ceperley, B. J. Alder, Phys. Rev. Letters **45**, 566 (1980)

83. J. C. Slater, Phys. Rev. **81**, 385 (1951)

84. M. A. Whitehead, in *Recent Advances in Density Functional Methods, Part II*, edited by D. P. Chong, World Scientific, Singapore (1997)

85. P. Ziesche, S. Kurth, J. P. Perdew, Comp. Mater. Sci. **11**, 122 (1998)

86. J. P. Perdew, Y. Wang, Phys. Rev. B **33**, 8800 (1986)

87. J. P. Perdew, Phys. Rev. B **33**, 8822 (1986)

88. A. D. Becke, Phys. Rev. A **38**, 3098 (1988)

89. C. Lee, W. Yang, R. G. Parr, Phys. Rev. B **37**, 785 (1988)

90. I-H. Lee, R. M. Martin, Phys. Rev. B **56**, 7197 (1997)

91. M. Ernzerhof, in *Density Functionals: Theory and Applications*, edited by D. Joubert, Springer-Verlag, Berlin (1998)

92. A. D. Becke, J. Chem. Phys. **98**, 5648 (1993)

93. A. D. Becke, J. Chem. Phys. **104**, 1040 (1996)

94. A. D. Becke, J. Chem. Phys. **107**, 8554 (1997)

95. J. Baker, M. Muir, J. Andzelm, A. Scheiner, in *Chemical Applications of Density-Functional Theory*, edited by B. B. Laird, R. B. Ross and T. Ziegler, ACS, Washington, DC (1996)

96. C. W. Bauschlicher Jr., A. Ricca, H. Partridge, S. R. Langhoff, in *Recent Advances in Density Functional Methods, Part II*, edited by D. P. Chong, World Scientific, Singapore (1997)

97. A. D. Becke, J. Chem. Phys. **109**, 2092 (1998)

98. I. R. Levine, *Quantum Chemistry*, 4th Edition, Prentice-Hall, New Jersey (1991)

99. E. J. Baerends, O. V. Gritsenko, R. van Leeuwen, in *Chemical Applications of Density-Functional Theory*, edited by B. B. Laird, R. B. Ross and T. Ziegler, ACS, Washington, DC (1996)

100. E. Wimmer, in *Density Functional Methods in Chemistry*, edited by J. K. Labanowski and J. W. Andzelm, Springer-Verlag, New York (1991)

101. J. F. Janak, Phys. Rev. B **18**, 7165 (1978)

102. A. St-Amant, D. R. Salahub, Chem. Phys. Letters **169**, 387 (1990)

103. D. R. Salahub, R. Fournier, P. Mlynarski, I. Papai, A. St-Amant, J. Ushio, in *Density Functional Methods in Chemistry*, edited by J. K. Labanowski and J. W. Andzelm, Springer-Verlag, New York (1991)

104. A. St-Amant, Ph. D. Thesis, University of Montreal (1992)

105. T. H. Dunning Jr., J. Chem. Phys. **90**, 1007 (1989)

106. D. E. Woon, T. H. Dunning Jr., J. Chem. Phys. **98**, 1358 (1993)

107. N. Godbout, D. R. Salahub, J. Andzelm, E. Wimmer, Can. J. Chem. **70**, 560 (1992)

108. E. Clementi, D. L. Raimondi, J. Chem. Phys. **38**, 2686 (1963)

109. D. E. Woon, T. H. Dunning Jr., J. Chem. Phys. **103**, 4572 (1995)

110. *Landolt-Börnstein Numerical Data and Functional Relationship in Science and Technology, New Series, Group II*, edited by O. Madelung (Springer, Berlin, 1992) Vol. 21

111. C. L. Pekeris, Phys. Rev. **112**, 1649 (1958)

112. W. L. Jolly, K. D. Bomben, C. J. Eyermann, At. Data Nucl. Data Tables **31**, 433 (1984)

113. K. A. Peterson, T. H. Dunning Jr., J. Phys. Chem. **99**, 3898 (1995)

114. *Landolt-Börnstein Numerical Data and Functional Relationship in Science and Technology, New Series, Group II*, edited by O. Madelung (Springer, Berlin, 1992) Vol. 19c

115. W. Caminati, R. Meyer, M. Oldani, F. Scappini, J. Chem. Phys. **83**, 3729 (1985)

116. M. J. S Dewar, E. G. Zoebisch, E. F. Healy, J. Amer. Chem. Soc. **107**, 3902 (1985)

117. WinMOPAC, Version 2.0, Fujitsu Limited, Chiba, Japan (1998)

118. T. H. Dunning Jr., private communication

119. M. E. Casida, C. D. Paul, A. Goursot, A. Koester, L. Petterson, E. Proynov, A. St-Amant, D. R. Salahub, H. Duarte, N. Godbout, J. Guan, C. Jamorski, M. Leboeuf, V. Malkin, O. Malkina, F. Sim, A. Vela, deMon-KS Version 3.4, deMon Software, University of Montreal (1997)

120. E. I. Proynov, E. Ruiz, A. Vela, D. R. Salahub, Int. J. Quant. Chem. Symp. **29**, 61 (1995)

121. E. Proynov, A. Vela, D. R. Salahub, Phys. Rev. A **50**, 3766 (1994)

122. D. P. Chong, S. R. Langhoff, J. Chem. Phys. **93**, 570 (1990)

123. D. P. Chong, Can. J. Chem. **73**, 79 (1995)

124. T. D. Thomas, J. Chem. Phys. **52**, 1373 (1970)

125. U. Gelius, C. J. Allan, G. Johansson, H. Siegbahn, D. A. Allison, K. Siegbahn, Phys. Scrypta **3**, 237 (1971)

126. D. W. Davis, *PhD Thesis*, University of California, Berkeley (1973)

127. T. D. Thomas, R. W. Shaw Jr., J. Electron Spectrosc. Rel. Phenom. **5**, 1081 (1974)

128. T. Ohta, T. Fujikawa, H. Kuroda, Bull. Chem. Soc. Japan **48**, 2017 (1975)

129. S. A. Holmes, T. D. Thomas, J. Amer. Chem. Soc. **97**, 2337 (1975)

130. B. Lindberg, S. Svensson, P.-A. Malmquist, E. Basilier, U. Gelius, K. Siegbahn, *Uppsala University Institute of Physics Report UUIP-910*, (1975)

131. W. B. Perry, W. L. Jolly, Inorg. Chem. **13**, 1211 (1974)

132. J. J. Pireaux, S. Svensson, E. Basilier, P.-A. Malmquist, U. Gelius, R. Caudano, K. Siegbahn, Phys. Rev. A **14**, 2133 (1976)

133. K. Siegbahn, C. Nordling, G. Johansson, J. Hedman, P. F. Heden, K. Harim, U. Gelius, T. Bergmark, L. O. Werme, R. Manne, Y. Baer, *ESCA Applied to Free Molecules*, North-Holland Publishing Company, Amsterdam (1969)

134. T. D. Thomas, J. Chem. Phys. **53**, 1744 (1970)

135. G. Johansson, J. Hedman, A. Berndtsson, M. Klasson, R. Nilsson, J. Electron Spectrosc. Rel. Phenom. **2**, 295 (1973)

136. S. R. Smith, T. D. Thomas, J. Electron Spectrosc. Rel. Phenom. **8**, 45 (1976)

137. W. L. Jolly, W. B. Perry, unpublished data quoted in reference 112

138. T. D. Thomas, J. Amer. Chem. Soc. **92**, 4184 (1970)

139. S. A. Holmes, *MS Thesis*, Oregon State University (1974)

140. T. Ohta, H. Kuroda, Bull. Chem. Soc. Japan **49**, 2939 (1976)

141. C. J. Allan, U. Gelius, D. A. Allison, G. Johansson, H. Siegbahn, K. Siegbahn, J. Electron Spectrosc. Rel. Phenom. **1**, 131 (1972)

142. K. Siegbahn, J. Electron Spectrosc. Rel. Phenom. **5**, 3 (1974)

143. D. W. Davis, J. M. Hollander, D. A. Shirley, T. D. Thomas, J. Chem. Phys. **52**, 3295 (1970)

144. D. W. Davis, D. A. Shirley, T. D. Thomas, in *Electron Spectroscopy*, edited by D. A. Shirley, North-Holland Publishing Company, Amsterdam (1972)

145. M. Barber, P. Baybutt, J. A. Conner, I. H. Hillier, W. N. E. Meredith, V. R. Saunders, in *Electron Spectroscopy*, edited by D. A. Shirley, North-Holland Publishing Company, Amsterdam (1972)

146. T. Fujikawa, T. Ohta, H. Kuroda, Bull. Chem. Soc. Japan **49**, 1486 (1976)

147. J. M. Buschek, F. S. Jorgensen, R. S. Brown, J. Amer. Chem. Soc. **104**, 5019 (1982)

148. D. B. Beach, C. J. Eyermann, S. P. Smith, S. F. Xiang, W. L. Jolly, J. Amer. Chem. Soc. **106**, 536 (1984)

149. P. Finn, R. K. Pearson, J. M. Hollander, W. L. Jolly, Inorg. Chem. **10**, 378 (1971)

150. R. S. Brown, A. Tse, J. Amer. Chem. Soc. **102**, 5222 (1980)

151. T. X. Carroll, S. R. Smith, T. D. Thomas, J. Amer. Chem. Soc. **97**, 659 (1975)

152. B. E. Mills, R. L. Martin, D. A. Shirley, J. Amer. Chem. Soc. **98**, 2380 (1976)

153. S. R. Smith, T. D. Thomas, J. Amer. Chem. Soc. **100**, 5459 (1978)

154. W. L. Jolly, unpublished data quoted in reference 112

155. H. W. Chen, W. L. Jolly, T. H. Lee, unpublished data quoted in reference 112

156. A. P. Hitchcock, M. Pocock, C. E. Brion, M. S. Banna, D. C. Frost, C. A. McDowell, B. Wallbank, J. Electron Spectrosc. Rel. Phenom. **13**, 345 (1978)

157. R. L. Martin, B. E. Mills, D. A. Shirley, J. Chem. Phys. **64**, 3690 (1976)

158. K. D. Bomben, W. L. Jolly, unpublished data quoted in reference 112

Appendix

It was pointed out in Chapter 5 that calculations using the ΔE-KS approach were initially limited to a database of reliable observed CEBEs which was selected in order to reduce as much as possible the effect of experimental errors on the assessment of functional performance.

The database consisted of seventeen cases, for each of which at least four experimental CEBEs have been documented. The experimental uncertainty δ was sometimes reported along with each observed value. Where δ was not given, a reasonable estimate was assumed.

Table A-1 summarizes the data for the seventeen cases which were studied in Chapter 5. Additional cases were considered for the basis-set tests reported in Chapter 6, and where experimental results were available, weighted averages were obtained, the corresponding data being given in Tables A-2 and A-3.

Table A-1. Observed $1s$ energies (in eV) for the molecules in the seventeen-case database.

molecule	year	CEBE	δ	average	weighted average	reference
C O	1969	295.9	0.2 [a]			133
	1970	296.2	0.1 [a]			134
	1973	296.1 [b]	0.1 [a]			133, 135
	1974	296.2	0.1 [a]			127
	1976	296.24	0.03			136
	1984	296.19	0.05 [a]			137
				296.14	296.21	
CO_2	1969	297.5	0.2 [a]			133
	1972	297.5	0.1			133, 141
	1973	297.69	0.14			135
	1974	297.69	0.14 [a]			142
	1974	297.75	0.07			127, 143
	1974	297.71	0.05			127
				297.64	297.69	
CH_4	1969	290.7	0.2 [a]			133
	1970	290.8	0.1			124
	1974	290.73	0.2 [a]			131
	1974	290.91	0.05			127
	1976	290.83	0.02			132
	1984	290.90 [c]	0.05 [a]			112, 131
				290.81	290.84	

Table A-1 continued

molecule	year	CEBE	δ	average	weighted average	reference
CF_4	1969	301.8	0.2 [a]			133
	1970	301.8	0.1 [a]			138
	1974	301.68	0.2 [a]			131
	1974	301.9	0.2			127, 144
	1974	301.96	0.05 [a]			127
	1984	301.85 [c]	0.05			112, 131
				301.83	301.89	
CCl_4	1970	296.3	0.1 [a]			138
	1974	296.22	0.2 [a]			131
	1974	296.38	0.05 [a]			139
	1976	296.3	0.1 [a]			140
	1984	296.39 [c]	0.05 [a]			112, 131
				296.32	296.36	
C_2H_6	1970	290.6	0.1 [a]			124
	1974	290.57	0.3 [a]			131
	1974	290.76	0.05 [a]			126, 127
	1976	290.71	0.02			132
	1984	290.74 [c]	0.05 [a]			112, 131
				290.68	290.72	
N_2	1969	409.9	0.2 [a]			133
	1973	409.93	0.10			135
	1974	409.95	0.20			127, 143
	1974	409.93	0.20			142
	1974	409.93	0.05			127
	1980	410.0	0.03			150
				409.94	409.98	

Table A-1 continued

molecule	year	CEBE	δ	average	weighted average	reference
NNO	1969	412.5	0.2 [a]			133
	1974	412.62	0.21			127, 143
	1974	412.5	0.1 [a]			127, 149
	1974	412.62	0.05 [a]			126, 127
				412.56	412.59	
NNO	1969	408.5	0.2 [a]			133
	1974	408.75	0.22			127, 143
	1974	408.6	0.1 [a]			127, 149
	1974	408.75	0.05 [a]			126, 127
				408.65	408.71	
CH_3CN	1972	405.9	0.3			145
	1976	405.6	0.2 [a]			146
	1982	405.74	0.03			147
	1984	405.60	0.02			148
				405.71	405.64	
CO	1969	542.1	0.5 [a]			133
	1970	542.3	0.1 [a]			134
	1973	542.6 [b]	0.1 [a]			133, 135
	1974	542.82	0.12 [a]			127, 143
	1976	542.40	0.11 [a]			155
	1976	542.57	0.03			136
	1984	542.51 [c]	0.05 [a]			112, 155
				542.47	542.55	

Table A-1 continued

molecule	year	CEBE	δ	average	weighted average	reference
$C\mathbf{O}_2$	1969	540.8	0.5 [a]			133
	1972	541.1	0.1			141
	1973	541.28	0.12			135
	1974	541.28	0.12			142
	1974	541.32	0.05			127
	1974	541.32	0.09			127, 143
				541.18	541.28	
$H_2\mathbf{O}$	1969	539.7	0.2 [a]			133
	1974	539.88	0.07			127
	1974	539.93	0.05 [a]			142
	1976	539.67	0.2 [a]			133, 152
				539.80	539.90	
HC**O**OH	1974	538.93	0.09			127, 143
	1975	538.92	0.05 [a]			153
	1976	538.75	0.2 [a]			133, 152
	1978	539.00	0.03			153
				538.90	538.97	
HCO**O**H	1974	540.55	0.09			127, 143
	1975	540.60	0.1 [a]			151
	1976	540.45	0.2 [a]			133, 152
	1978	540.65	0.03			153
				540.56	540.63	
$CH_3\mathbf{O}H$	1969	538.9	0.2 [a]			133
	1974	539.08	0.12			127, 143
	1976	539.09	0.08			127, 152
	1984	539.2	0.1 [a]			154
				539.07	539.11	

Table A-1 continued

molecule	year	CEBE	δ	average	weighted average	reference
CF_4	1969	695.2	0.2 [a]			133
	1970	695.0	0.1 [a]			138
	1973	695.52	0.14			135
	1974	695.60	0.2 [a]			131
	1974	695.52	0.14			142
	1974	695.52	0.05 [a]			139
	1974	695.57	0.05			127
	1984	695.77 [c]	0.05 [a]			112, 131
				695.46	695.56	

[a] assumed

[b] recalibrated, based on the improved measurement on CO_2 [135]

[c] correction applied according to reference 112

Table A-2. Observed 1*s* energies (in eV) for the aromatic compounds in Table 6-6.

molecule	year	CEBE	δ	average	weighted average	reference
$\mathbf{C}_6H_6$	1970	290.4	0.1 [a]			124
	1971	290.2	0.1			125
	1974	290.42	0.05 [a]			126, 127
	1975	290.3	0.2			128
	1975	290.38	0.07			129
	1975	290.42	0.05[a]			130
				290.35	290.39	
$\mathbf{C}_6H_5NH_2$	1975	291.38	0.05 [a]			130
	1975	291.2	0.2			128
				291.38	291.37	
$\mathbf{C}_6H_5F$	1975	292.85	0.05 [a]			130, 144
	1975	292.70	0.05 [a]			130
	1975	292.9	0.2			128
	1978	292.5	0.1			156
				292.74	292.75	
$C_6H_5\mathbf{N}H_2$	1969	405.5	0.1 [a]			133
	1975	405.32	0.05 [a]			130
	1975	405.3	0.2			128
	(?)	405.31	0.05 [a]			112
	1980	405.45	0.03			150
				405.38	405.40	
$C_6H_5\mathbf{F}$	1974	692.88	0.05 [a]			139, 144
	1975	692.93	0.05 [a]			130
	1975	693.3	0.2			128
				693.04	692.92	

[a] assumed

Table A-3. Observed 1*s* energies (in eV) for hydrogen fluoride.

molecule	year	CEBE	δ	average	weighted average	reference
H**F**	1974	694.22	0.05 [a]			127
	1976	694.0	0.2			157
	1984	694.31	0.1 [a]			112, 158
				694.18	694.23	

[a] assumed